# Design, synthesis and application of sulfur-containing heterocycles for the inhibition of glycosidases and glycosyltransferases

Kok, K.

# 2

# 1,6-*epi*-Cyclophellitol Cyclosulfamidate Is a Bona Fide Lysosomal α-Glucosidase Stabilizer for the Treatment of Pompe Disease

*Manuscript published as:*

Ken Kok, Chi-Lin Kuo, Rebecca E. Katzy, Lindsey T. Lelieveld, Liang Wu, Véronique Roig-Zamboni, Gijsbert A. van der Marel, Jeroen D. C. Codée, Gerlind Sulzenbacher, Gideon J. Davies, Herman S. Overkleeft, Johannes, F. M. G. Aerts, Marta Artola, *J .Am. Chem. Soc.* **2022**, *144*, 14819-14827.

## 2.1 Introduction

Acid maltase, also known as human acid α-glucosidase (GAA, EC 3.1.1.20), is a retaining exo-α-glucosidase part of the CAZy GH31 glycoside hydrolase family (http://www.cazy.org). This α-glucosidase is responsible for the degradation of glycogen by cleaving a terminal glucose moiety from the polysaccharide.[1,2] Mutations in the gene that encodes for GAA can lead to enzyme deficiency which consequently can produce multiple phenotypic forms of Pompe disease (PD).[3,4] PD is a lysosomal storage disorder (LSD) characterized by a lysosomal accumulation of glycogen, which ultimately causes a progressive disfunction and apoptosis in cardiac and skeletal muscle tissue leading towards loss of respiratory and cardiac motor functions.[5,6,7]

The current golden standard for the treatment of PD patients consists of enzyme replacement therapy (ERT) in which a patient receives an intravenous injection of recombinant human rhGAA (alglucosidase alpha, Myozyme® (ex-US) or Lumizyme® (US)).[8,9] The downside of this treatment predominantly originates from the inefficient trafficking and lysosomal delivery of the recombinant enzymes due to their limited plasma stability and autophagic accumulation within Pompe skeletal muscle tissue.[10,11] Therefore, only a fraction of the administered enzyme reaches its correct destination: muscle tissue. The efficacy of the treatment is further affected by the recruitment of host-antibodies against the recombinant enzyme.[12,13] To circumvent these problems an alternative therapeutic intervention was developed for the treatment of LSDs, which is called pharmacological chaperone therapy (PCT). In PCT, small reversible molecular chaperones are used to occupy the native enzyme active site in a reversible manner, thereby stabilizing the mature protein fold and helping the protein to surpass the quality control machinery of the endoplasmic reticulum (ER) and facilitating its transport towards the lysosomes. However, only a small part of the PD patients have mutations that are susceptible towards PCT.[14] More recently, the combination of ERT and PCT has shown to be more effective in murine Pompe models than either of the individual therapeutic modalities.[15] PCT using the iminosugars deoxynojirimycin (DNJ **1**, Duvoglustat) or *N*-butyldeoxynojirimycin (NB-DNJ **2**, Miglustat) has been in clinical trials for the last decade, either as a combination therapy with ERT or as a monotherapy.[16,17,18] More recently, ERT (Cipaglucosidase alfa from Amicus Therapeutics) combined with NB-DNJ was approved in March 2023 for the treatment of adults with late-onset Pompe disease in the European Union.[19] However, both these iminosugars are not selective for GAA and also target an array of other glycosidases including GBA1, GBA2

and glucosylceramide synthase (GCS).[20] A small group of reversible GAA inhibitors has been described in the past. *N*-acetylcysteine is an allosteric positive modulator able to stabilize rhGAA, although it does so at concentrations (10 mM) that might not be therapeutically relevant.[21,22] A set of *in vitro* rhGAA activators were described by Marugan *et al.* more than a decade ago for which the stabilization mechanism and binding mode remain to be investigated.[23] More recently, Kato and collaborators described a set of *C*-branched arabinose- and glucose-configured iminosugars able to inhibit rhGAA *in vitro* at nanomolar concentrations.[24,25] The most advanced inhibitor, 5-*C*-heptyl-deoxynojirimycin, despite having displayed a nanomolar $IC_{50}$, stabilizes rhGAA in Pompe fibroblasts at 10 μM, and its selectivity towards other glycosidases has not been yet determined. This inhibitor illustrates that high *in vitro* inhibitory potencies do not necessarily correlate with an optimal enzyme stabilization. In principle, the ideal pharmacological chaperone in a combined chaperone-ERT setting, binds and stabilizes, recombinant enzyme (here rhGAA) in circulation but is outcompeted by its natural substrate (here lysosomal glycogen) upon reaching its (sub)cellular target. The fine-tuning of this inhibition/binding *versus* an optimal stabilization effect can therefore not be predicted by low *in vitro* inhibitory constants.

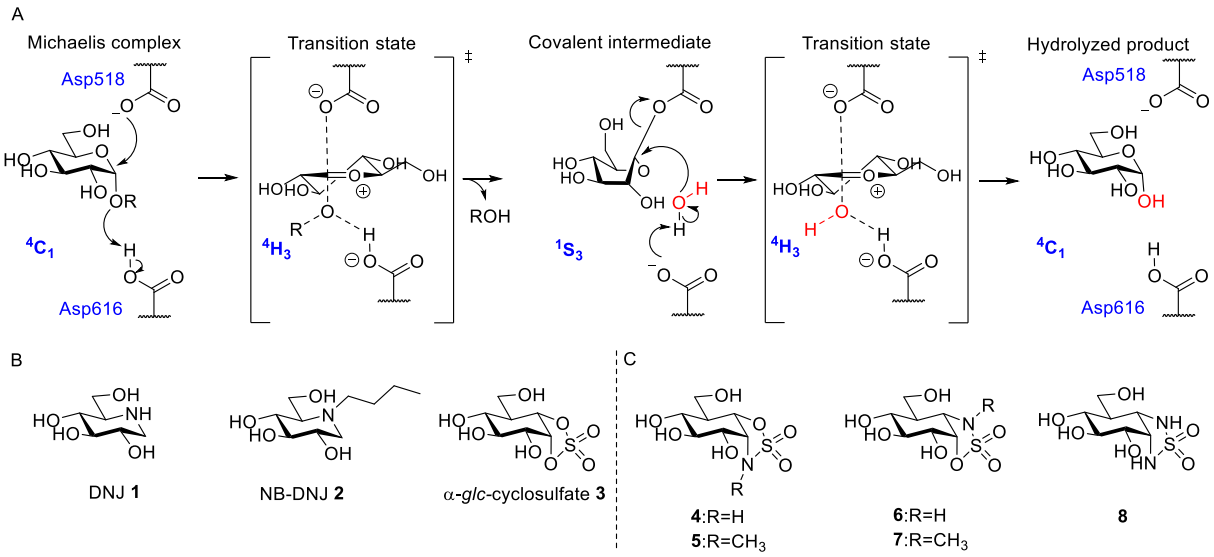


**Figure 2.1.** α-Glucosidase mechanism and chemical structures of α-glucosidase inhibitors. A) Koshland double displacement mechanism of α-glucosidases. B) Deoxynojirimycin (DNJ **1**, Duvoglustat), *N*-butyldeoxynojirimycin (NB-DNJ **2**, Miglustat) and 1,6-*epi*-cyclophellitol cyclosulfate **3**. C) New α-D-glucose configured cyclosulfamidates **4**-**7** and cyclosulfamide **8**.

Retaining α-glucosidases employ a conserved two step Koshland double displacement mechanism, in which α-glucosidase residues are hydrolysed by two key carboxylic acid residues functioning as catalytic nucleophile (Asp518 in GAA and Asp412 in *Cj*Agd31B, a

bacterial homologue of GAA) and catalytic acid/base (Asp616 in GAA and Asp480 in *Cj*Agd31B) (Figure 2.1A). Recently, 1,6-*epi*-cyclophellitol cyclosulfate **3** (Figure 2.1B) has been described as a potent and irreversible α-glucosidase inhibitor, which gains selectivity over β-glucosidases by mimicking the $^4C_1$ Michaelis complex conformation adopted by α-glucoside substrates within the enzyme active site upon the start of the hydrolysis catalysed by an aspartic acid residue (Asp518 in GAA).[26] This cyclic sulfate has shown superior reactivity and regioselectivity compared to the epoxide and aziridine derivatives.[26] In addition, previous work where a non-hydrolysable cyclopropyl group was introduced as a replacement of the epoxide or aziridine demonstrated that conformational mimicry of a transition state is just as important as the electrophilicity of the introduced moieties for the inhibition of α-glucosidases.[27] Based on these previous studies, α-galactose-configured cyclophellitol cyclosulfamidates were developed as conformational reversible inhibitors suitable for PCT in combination with recombinant α-galactosidase A (α-GalA) for the treatment for Fabry disease.[28] These sulfamidates were designed with the aim of reducing the electrophilicity of the cyclic sulfate system by replacing one of the endocyclic oxygen atoms for a nitrogen atom so that the covalent attachment of the enzyme could be prevented. The C-N bonds are less polarized compared to the C-O bonds which caused a reduction of the electrophilicity of the sulfamidates compared to the cyclic sulfates. This α-gal-cyclosulfamidate, also a $^4C_1$ Michaelis complex mimetic, and although less effective than commercial Migalastat, turned out to be an effective reversible α-galactosidase A (α-GalA) inhibitor able to stabilize α-GalA *in vitro* and *in cellulo* at high micromolar concentrations and is an optimal candidate for the treatment of Fabry disease.[28] Both α-GalA and GAA utilize an identical enzymatic reaction mechanism following $^4C_1$ (Michaelis) → $[^4H_3]^‡$ → $^1S_3$ (covalent intermediate) → $[^4H_3]^‡$ → $^4C_1$ (product) as substrate conformational itineraries. Based on the reversibility and the enzyme stabilization effect of the α-*gal*-cyclosulfamidate as well as the nanomolar inhibition of GAA by α-*glc*-cyclosulfate **3**, α-*glc*-cyclosulfamidates were envisioned as potential competitive GAA inhibitors and enzyme stabilizers for the treatment of PD. In this chapter the synthesis and biological evaluation of 1,6-*epi*-cyclophellitol cyclosulfamidates **4**-**7** and sulfamide **8** are described, and their mechanism of action, their potential as reversible inhibitors for lysosomal, ER and intestinal α-glucosidases as well as their superiority over commercially available NB-DNJ **2** as (recombinant) enzyme stabilizers are investigated.

## 2.2 Results and Discussion

### 2.2.1 Design and synthesis of Human acid α-glucosidase inhibitors

Giving the similarity in the substrate conformational itineraries of α-GalA and GAA it was predicted that *glc*-cyclosulfamidates **4**-**7** or cyclic sulfamide **8** with α-stereochemistry at the pseudo-anomeric position could lead to effective reversible GAA inhibitors. The synthesis of sulfamidates **4**-**7** was started by the nucleophilic addition of sodium azide to tetra-*O*-benzyl cyclophellitol **9** to obtain a mixture of *trans*-azido alcohols **10** and **19**.[29] These azides were separated by silica gel column chromatography and subsequently reduced to *trans*-amino alcohols **11** and **20** by hydrogenation using $PtO_2$, also known as Adam's catalyst, in excellent yields (Scheme 2.1A and 2.1B). Similar results could be obtained by Staudinger reduction of the respective azides using triphenylphosphine on resin. *N*-Boc protection of **11** followed by mesylation of the remaining free hydroxyl of **12** yielded fully protected mesylate **13** as the sole product. This in contrast to the mesylation of compound **21**, which also resulted in the formation of *trans*-oxazolidinone **32** potentially due to double-inversion caused by 1-methylimidazole (Scheme S2.1). Compounds **13** and **22** were both heated to 120 ℃ to initiate neighboring-group participation of the *N*-Boc group, which through displacement of the mesylates afforded *cis*-oxazolidinones **14** and **23**. The cyclic carbamate moieties of both compounds were subjected to basic hydrolysis to obtain the desired *cis*-amino alcohols **15** and **24**, respectively. Boc protection of the respective amines followed by cyclisation using thionyl chloride resulted in the formation of cyclic sulfite intermediates. Oxidation of these sulfites, using $RuCl_3$ and $NaIO_4$ to form $RuO_4$ *in situ*, afforded fully protected α-*glc*-cyclosulfamidates **16** and **25**. After acidic removal of the Boc protecting group and benzyls using standard hydrogenation conditions target compounds **4** and **6** were obtained. To investigate if GAA could accommodate cyclic sulfamidate moieties with additional functionalization at the endocyclic nitrogens, cyclosulfamidates **5** and **7** were synthesized. This was achieved by alkylating Boc-deprotected intermediates **17** and **26** using methyl iodide under basic conditions to afford the fully protected methylated sulfamidates **18** and **27**. After global deprotection, the desired methylated analogues **5** and **7** were obtained. Finally, α-*glc*-cyclosulfamide **8** was synthesized from trans-azido alcohol **19**, since as previously mentioned, subsequent mesylation of azido alcohol **10** and treatment with sodium azide could lead to elimination of the mesylate. Following this route, mesylate **28** was successfully converted to diazido-compound **29**. Both azides were hydrogenated to obtain diamine **30** which after cyclisation using sulfamide under basic conditions afforded protected

cyclosulfamide **31**. This intermediate was finally debenzylated to afford α-*glc*-cyclosulfamide **8**.

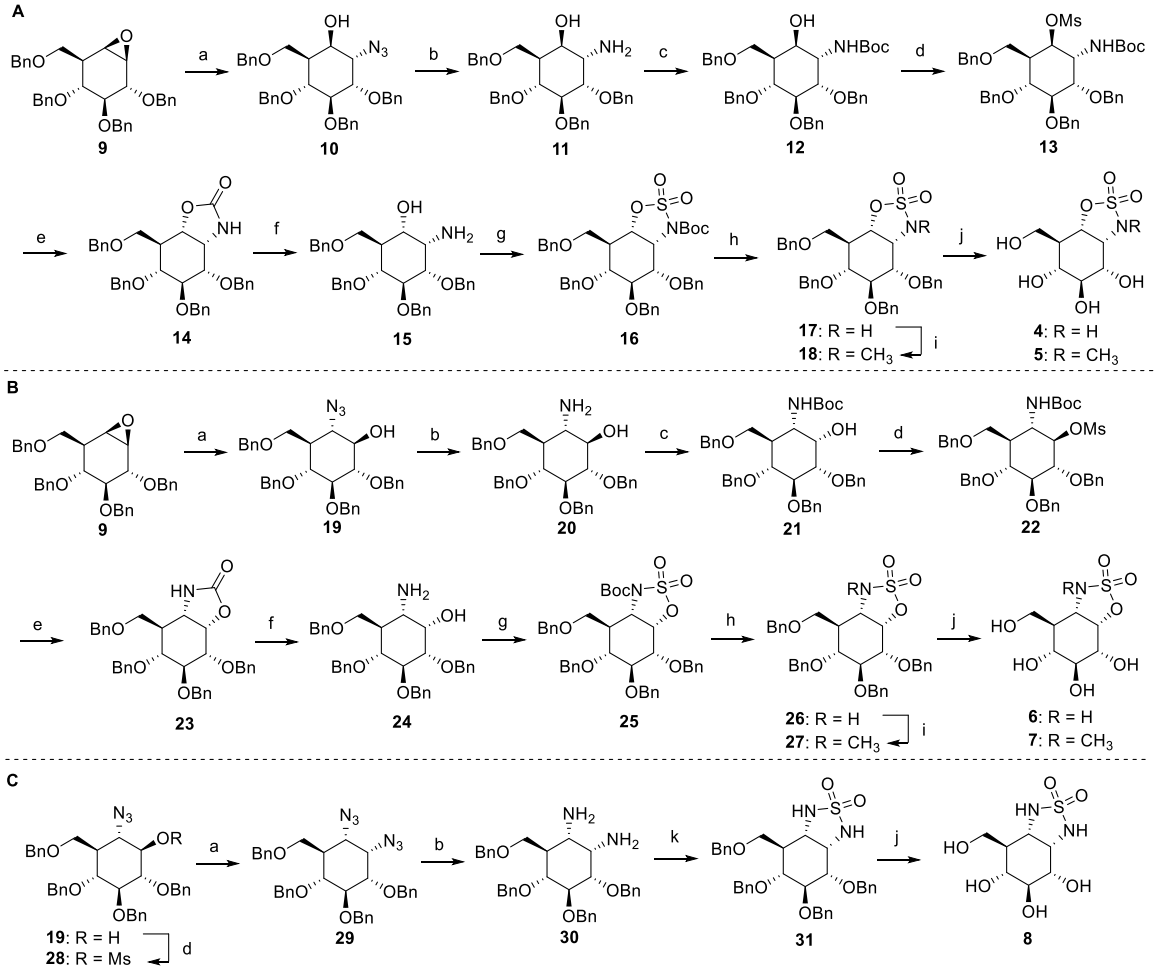

**Scheme 2.1.** Synthesis of cyclosulfamidates **4** and **5** (A), cyclosulfamidates **6** and **7** (B) and cyclosulfamide **8** (C). Reagents and conditions: (a) $NaN_3$, DMF, 18 h, 38% (**10**), 34% (**19**), 71% (**29**); (b) $PtO_2$, $H_2$, THF, rt, 18 h, 98% (**11**), 97% (**20**), 92% (**30**); (c) $Boc_2O$, $Et_3N$, DCM, 18 h, rt, 82% (**12**), 78% (**21**); (d) MsCl, Me-imidazole, $Et_3N$, $CHCl_3$, 5 h, rt, 91% (**13**), 80% (**22**), 88% (**28**); (e) DMF, 24 h, 120 ℃, 64% (**14**), 85% (**23**); (f) 1M NaOH, EtOH, 70 ℃, 18 h, 96% (**15**), 82% (**24**); (g) *i:* $Boc_2O$, $Et_3N$, DCM, rt, 18 h; *ii:* $SOCl_2$, $Et_3N$, imidazole, DCM, 15 min, 0 ℃; iii: $RuCl_3$, $NaIO_4$, 1:1:1 $H_2O$, EtOAc, MeCN, 1h, 0 ℃, 77% (**16**), 33% (**25**) over 3 steps; (h) TFA, DCM, rt, 1 h, 62% (**17**), 65% (**26**); (i) MeI, $K_2CO_3$, TBAI, 18 h, rt, 65% (**18**), 79% (**27**); (j) Pd/C, $H_2$, MeOH, rt, 18 h, 99% (**4**), 55% (**5**), 87% (**6**), 89% (**7**), 96% (**8**); (k) sulfamide, pyridine, reflux, 6 h, 91%.

### 2.2.2 *In vitro* inhibition of Human Acid α-glucosidase

Apparent half-maximal inhibitory concentration ($IC_{50}$) values were determined to assess the inhibitory potency of **4**-**8** against lysosomal α-glucosidase (GAA) and ER α-glucosidase II (GANAB) as well as the selectivity of the compounds over human β-glucosidases GBA1, GBA2 and glycosyltransferase GCS. Compounds **4**-**8** were compared to known GAA inhibitors NB-DNJ **2** and α-*glc*-cyclosulfate **3** and the $IC_{50}$ values were determined *in vitro* by measuring

processing inhibition of the respective (alpha and beta) 4-methylumbelliferyl (4-MU)-D-glucopyranoside fluorogenic substrates, whereas GCS inhibition was evaluated in RAW 264.7 cells by measuring inhibitor-dependent glucosylation of C6-NBD-ceramide as the fluorescent substrate (Table 2.1.) Cyclosulfamidate **4** showed to be a low-micromolar inhibitor of GAA ($IC_{50}$ = 5.17 μM) and slightly more potent than the commercially available iminosugar **2** ($IC_{50}$ = 26.7 μM). Furthermore, cyclosulfamidate **4** exhibited excellent selectivity against potential off targets such as β-glucosidases GBA1 and GBA2, and the glycosyltransferase GCS. This was in contrast to NB-DNJ **2** which inhibited GBA2 ($IC_{50}$ = 957 nM) and GCS ($IC_{50}$ = 43 μM) rather potently. Methylated analogue **5** showed much weaker inhibition towards GAA ($IC_{50}$ = 485 μM) and was inactive towards GANAB which suggested that there is no room for functionalization at the endocyclic nitrogen. In comparison, sulfamidate **6**, with the endocyclic oxygen at the pseudo-anomeric position, was revealed to be a 10-fold less potent GAA inhibitor, with comparable inhibitory activity for GANAB ($IC_{50}$ = 112 and 54 μM, respectively). Methylation of sulfamidate **6** was somehow tolerated by GANAB ($IC_{50}$ = 132 μM) and sulfamidate **7** targeted GBA and GBA2 as well ($IC_{50}$ = 93 and 652 μM, respectively). Finally, as illustrated by sulfamide **8**, double substitution of the endocyclic oxygens of cyclic sulfate **3** by nitrogens was detrimental for α-glucosidase activity.

**Table 1.** Apparent $IC_{50}$ values for *in vitro* inhibition of Glucosyl processing enzymes. Reported values are mean ± standard deviation from 3 technical triplicates. N.D.: not determined.

| Cmp | *In vitro* GAA $IC_{50}$ (μM) | *In vitro* GANAB $IC_{50}$ (μM) | *In vitro* GBA $IC_{50}$ (μM) | *In vitro* GBA2 $IC_{50}$ (μM) | *In situ* GCS $IC_{50}$ (μM) |
|---|---|---|---|---|---|
| **2** | 26.7 ± 0.60 | 153 ± 21.5 | > 1000 | 0.957 ± 0.499 | 43.0 ± 3.60 |
| **3** | 0.048[a] ± 1.0 x $10^{-4}$ | 0.026[a] ± 0.004 | 838.1[b] | 62 % inhibition at 500 μM | N.D. |
| **4** | 5.17 ± 0.195 | 496 ± 30.0 | 0 % inhibition at 500 μM | 0 % inhibition at 500 μM | 0 % inhibition at 50 μM |
| **5** | 485 ± 146 | 6 % inhibition at 500 μM | 0 % inhibition at 500 μM | 393 ± 93.7 | N.D. |
| **6** | 112 ± 2.54 | 47.0 ± 1.75 | 0 % inhibition at 500 μM | 0 % inhibition at 500 μM | 0 % inhibition at 50 μM |
| **7** | > 1000 | 132 ± 11.8 | 93.4 ± 7.83 | 652 ± 87.3 | 0 % inhibition at 50 μM |
| **8** | > 500 | 0 % inhibition at 500 μM | > 500 | 0 % inhibition at 500 μM | 0 % inhibition at 50 μM |

[a]Values in accordance with ref 19.

The selectivity of sulfamidate **4** for α-glucosidases over β-glucosidases was further corroborated by competitive activity-based protein profiling (cABPP) in mouse intestine homogenates for which α-glucosidase Cy5-ABP **34**, broad spectrum β-glucosidase Bodipy green-ABP **35** and β-galactosidase Cy5-ABP **36** were used (Figure S2.1). This experiment demonstrated that both sulfamidate **4** and iminosugar **2** inhibit intestinal sucrase-isomaltase (SI) and maltase- glucoamylase (MGAM), which are intestinal α-glucosidases involved in food processing that have been extensively targeted to prevent and treat type II diabetes mellitus.[30,31] Notably, inhibition of gastrointestinal α-glucosidases with antidiabetic drugs has been related to undesired effects, including flatulence, diarrhoea, and abdominal pain. Cyclosulfamidate **4** inhibited SI and MGAM but did so about 100-fold less potently compared to its inhibition of rhGAA or GANAB, and therefore exhibited a better therapeutic window compared to NB-DNJ **2**. Sulfamidate **4** and NB-DNJ **2** also showed to be selective over both β-glucosidase and β-galactosidase activities of lactase-phlorizin hydrolase (LPH) (Figure 2.3**)**.

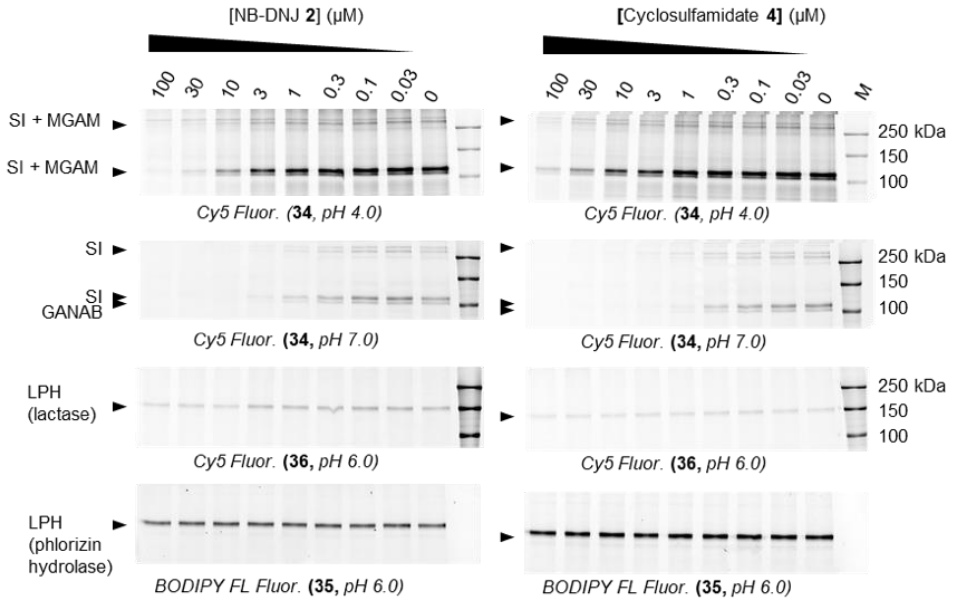


**Figure 2.3. Competitive ABPP (cABPP) in mouse intestine homogenates.** Mouse duodenum (60 μg protein) extracts were pre-incubated with cyclosulfamidate **4** or NB-DNJ **2** (0-100 μM) for 30 min at 37 ℃ at pH 4.0, 6.0 or 7.0 followed by labelling of sucrase-isomaltase (SI) and maltase-glucoamylase (MGAM) by Cy5 α-glucosidase ABP **34** (pH 4.0 or 7.0). Lactase pocket of lactase-phlorizin hydrolase (LPH) was labelled with Cy5 ABP **36** and phlorizin hydrolase pocket of LPH was labelled by pre-blocking the lactase pocket of LPH with β-galactosidase ABP **36** for 30 min at 37 ℃ at pH 6.0, followed by subsequent incubation with **4** and NB-DNJ **2**, and final labelling with green BODIPY β-glucosidase ABP **35** (See Figure S2.1 for ABP structures).

When looking at the inhibition kinetics, inhibitors **4** and **6** preincubated with Myozyme at concentrations of their corresponding apparent $IC_{50}$ values for different time periods (15, 30, 45, 60, 120, 180 and 240 min) indicated that sulfamidate **6** was an irreversible inhibitor (this was concluded due to a residual decrease of α-glucosidase activity observed after longer incubation times) (Figure 2.4B). This was in contrast to cyclosulfamidate **4** which showed a constant level of α-glucosidase activity indicating cyclosulfamidate **4** to inhibit rhGAA in a competitive manner (Figure 2.4A).

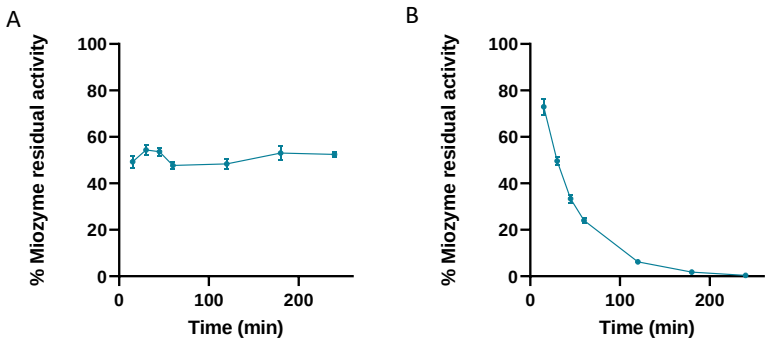


**Figure 2.4.** Time dependent inhibition of recombinant human acid α-glucosidase (rhGAA, Myozyme) by cyclosulfamidates **4** and **6**. Residual activity of rhGAA with different pre-incubation times (15, 30, 45, 60, 120, 180 and 240 min) in the presence of **4** (A) and **6** (B) at their *in vitro* apparent $IC_{50}$ concentrations (66 μM and 5.1μM respectively).

Kinetic parameters determined with increasing 4-MU-α-glucoside concentrations proved that **4** reversibly inhibits rhGAA with a $K_i$ of 3.40 μM, approximately 5-fold more potently than NB-DNJ **2** ($K_i$ 15.2 μM) (Table 2). In contrast, cyclosulfamidate **6** proved to be an irreversible inhibitor of GAA with a *Ki* of 378 μM and $k_{inact}$ of 0.35 $min^{-1}$.[28]

**Table 2.** Inhibition constants ($K_i$, $K_I$ and $k_{inact}$) in human recobinant α-glucosidase A rhGAA (Myozyme).

| **Compound** | Kinetic parameters in rhGAA |
|---|---|
| NB-DNJ **2** | $K_i$ = 15.2 μM |
| **4** | $K_i$ = 3.4 μM |
| **6** | $K_i$ = 456 μM and $k_{inact}$ = 0.35 $min^{-1}$ |

### 2.2.3 Structural characterization of enzyme-inhibitor complexes

Crystallographic studies with the proteolytically digested form of human recombinant rhGAA (Myozyme) (Figure 2.5A and B) and the bacterial GH31 α-glucosidase/transglucosidase CjAgd31B homologue from *Cellvibrio japonicus* (Figure 2.5C and D) further demonstrated the binding motifs of cyclosufamidates **4** and **6**.[22,32] The X-ray structure of human α-glucosidase rhGAA in complex with sulfamidate **4** revealed that the sulfamidate was able to bind within the active site of both enzymes by adopting a $^4C_1$ Michaelis-type conformation in a non-covalent manner (Figure 2.5A and C). The interactions of the cyclitol moiety of sulfamidate **4** with rhGAA were virtually identical to those observed in previously reported complex structures of rhGAA with GAA inhibitors, acarbose, 1-deoxynojirimycin (DNJ), and *N*-hydroxyethyl-DNJ (NHE-DNJ), notably with Asp443, Asp616, Asp645 and Trp481 (Figure 2.5A).[22] The endocyclic nitrogen of the sulfamidate established a tight hydrogen-bonding interaction with the acid/base Asp616. This provided a structural rational for the lack of inhibition observed for methylated analogue **5** due to steric hindrance. The endocyclic nitrogen and the sulfate moieties of sulfamidate **4** overlapped spatially with the nitrogen and substrate +1 aglycone atomic features, respectively, of acarvosine reported previously (Figure 2.5A).[22] This reinforced that sulfamidate **4** is a true substrate Michaelis complex mimetic for GAA. Structural data for the rhGAA-sulfamidate **6** complex clearly revealed that the cyclosulfamidate with the endocyclic oxygen atom attached to the pseudo-anomeric position acted as an electrophilic trap, yielding a covalent complex with the enzyme and adopting a final $^1S_3$ conformation in the enzyme active site after reacting with the catalytic nucleophile Asp518 (Figure 2.5B).[33] The interactions observed for the cyclitol moiety of **6** were essentially identical to those observed in the rhGAA-sulfamidate **4** complex, though the sulfamidate moiety engenders steric constraints on the active-site scaffold. The bulky sulfamidate, liberated from the cyclic restraint of the

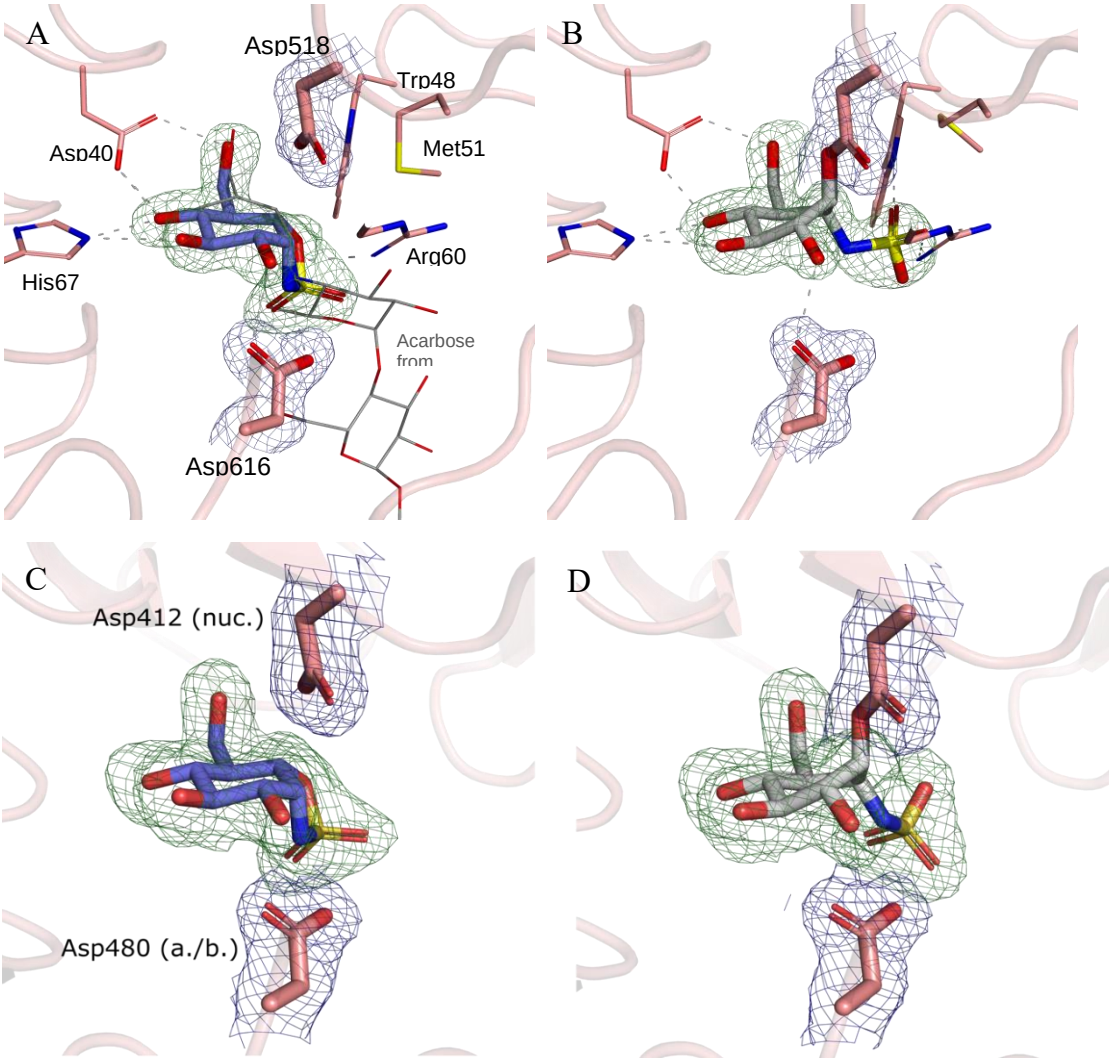


**Figure 2.5.** α-*Glc*-cyclosulfamidates **4** and **6** in complex with the proteolytically digested form of recombinant human rhGAA (Myozyme) (A and B) or bacterial homologue from *Cellvibrio japonicus* *Cj*Agd31B (C and D). (A) α-*Glc*-cyclosulfamidate **4** forms a $^{4}C_{1}$ non-reacted complex with rhGAA. (B) α-*Glc*-cyclosulfamidate **6** reacts covalently with rhGAA nucleophile (Asp518) adopting a final $^{1}S_{3}$ conformation. (C) *Cj*Agd31B forms a non-covalent complex with **4**, with the ligand adopting a $^{4}C_{1}$ conformation in the enzyme active site. (D) Cyclosulfamidate **6** reacts with *Cj*Agd31B, producing a $^{1}S_{3}$ covalent complex linked to the enzyme's nucleophilic residue (Asp412).

cyclophellitol framework, pushed outward Met519, Trp481 and the associated loop region (Figure 2.5B). The energy cost of this structural perturbation was compensated for by several H-bonding interactions between the sulfamidate and rhGAA active-site residues, pleading for stabilization of the abortive complex.

### 2.2.4 *In vitro, in cellulo and in vivo* stabilization of rhGAA

To investigate if **4** could function as a potential pharmacological chaperone, the ability of the sulfamidate to stabilize α-glucosidases *in vitro* and *in situ* was tested. Thermostability assays (TSAs) showed that α-*glc*-sulfamidate **4** stabilizes rhGAA with a maximum shift in inflection temperature ($\Delta Ti_{max}$) of 11.2 ℃ and a half maximal effective concentration ($EC_{50}$) of 1.16 μM, whereas α-*glc*-sulfamidate **6** did not prevent enzyme unfolding at increasing temperatures (Figure 2.6 and S2.1). Similar assays with *Cj*Agd31B using a Sypro Orange dye revealed that α-*glc*-sulfamidate **4** stabilized the bacterial analogue *in vitro* as well with a $\Delta Ti_{max}$ of 5.2 ℃ and an $EC_{50}$ of 134 μM (Figure S2.2 and S2.3).

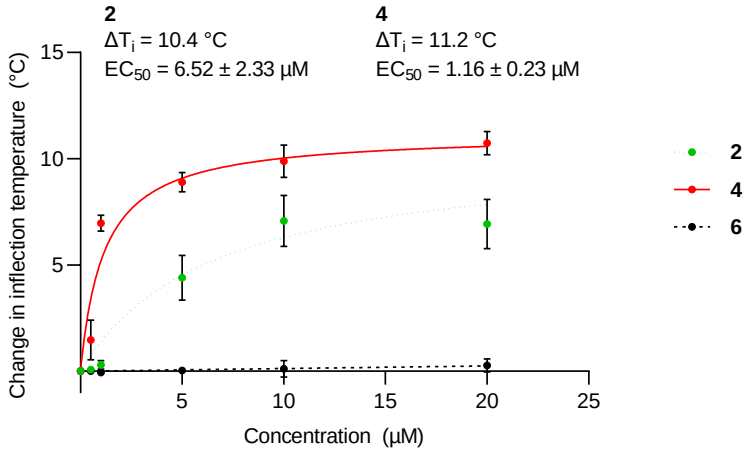


**Figure 2.6.** GAA activity in Pompe disease fibroblasts. A. The effect of **2**, **4** and **6** on the thermostability of rhGAA. The graph shows heat-induced denaturation profiles of rhGAA in complex with **2** (green), **4** (red) and **6** (black).

Prompted by these results, the stabilization effect of sulfamidate **4** on rhGAA (10 nM final concentration) was investigated in cell medium (Figure 2.7A) and in plasma (Figures 2.7B and 2.7C) from adult Pompe patients with almost no residual α-glucosidase activity. Stabilization experiments in cell medium showed that rhGAA was completely degraded in cell medium after 4 days incubation, which was reduced to 50% degradation by the addition of cyclosulfamidate **4** (20 μM), a significant improvement compared to the 5% remaining with NB-DNJ **2** (Figure 2.7A). In addition, the stabilization effect was further investigated in plasma from healthy individuals (Figure 2.7B) and two different Pompe patients: an adult Pompe patient with genotype: p. L355P; p. R672W under ERT (last infusion 11 days before sampling) and another adult Pompe patient with genotype: c.-32-13 T > G; p.N403K under no treatment (Figure 2.7C). In contrast to the cell medium, degradation of rhGAA in plasma occurred much faster, with more than 85% degradation after just 1 h. Addition of cyclosulfamidate **4** (20 μM) slowed such

degradation in plasma from healthy individuals and Pompe patients with a similar efficacy: more than 3-fold increase in rhGAA was observed after 2 h in plasma from an adult Pompe patient (Figure 2.7B and 2.7C). Of note, in this experiment, more than doubled stabilization effect was observed for cyclosulfamidate **4** compared to that of NB-DNJ **2**.

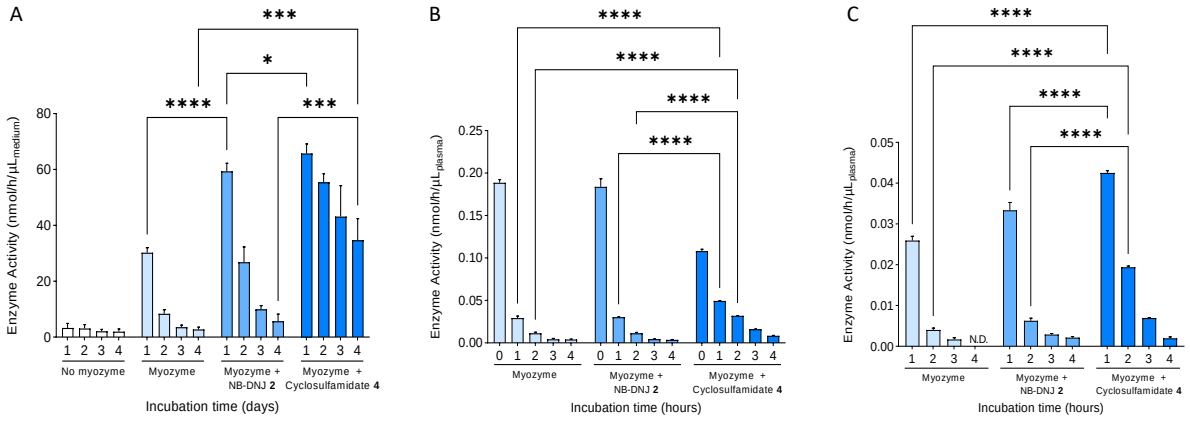


**Figure 2.7.** Myozyme (10 nM) was incubated in (A) cell culture medium, (B) plasma from healthy individuals or (C) plasma from an adult Pompe patient (genotype: p.L355P; p.R672W) under ERT (last infusion 11 days before sampling) for 1-4 days (in medium) or 1-4 hours (in plasma) in combination with or without 20 µM NB-DNJ **2** or cyclosulfamidate **4**. Experiment was performed in biological triplicates, N = 2 technical replicates. Data are depicted as mean ± SD and analyzed using a Two-Way ANOVA with Tuckey's multiple comparisons test. *$p < 0.05$.

Subsequently, two different cell passages of Pompe fibroblasts were incubated with either NB-DNJ **2** (at 20 µM) or cyclosulfamidate **4** (at 20 µM) in the presence or absence of rhGAA Myozyme (10 nM) for 1-3 days, and activity was measured every 24 h without refreshing the media (Figure 2.8). A two-fold increase of rhGAA activity was observed after 3 days-treatment of fibroblasts with the combination of rhGAA and **4** compared to fibroblasts treated only with rhGAA. This indicated that sulfamidate **4** was able to stabilize the enzyme in cells. This increase in rhGAA activity was also observed after longer incubations (from day 1 to day 3), which suggested that cyclosulfamidate **4** may stabilize the enzyme in the medium, making more enzyme available for cell internalization and transport towards the lysosomes. Stabilization experiments in cell medium showed that rhGAA was completely degraded in cell medium after 4 days incubation, which was reduced to 50% degradation by the addition of cyclosulfamidate **4** (20 µM), a significant improvement compared to the 5% remaining with NB-DNJ **2** (Figure 2.7A).

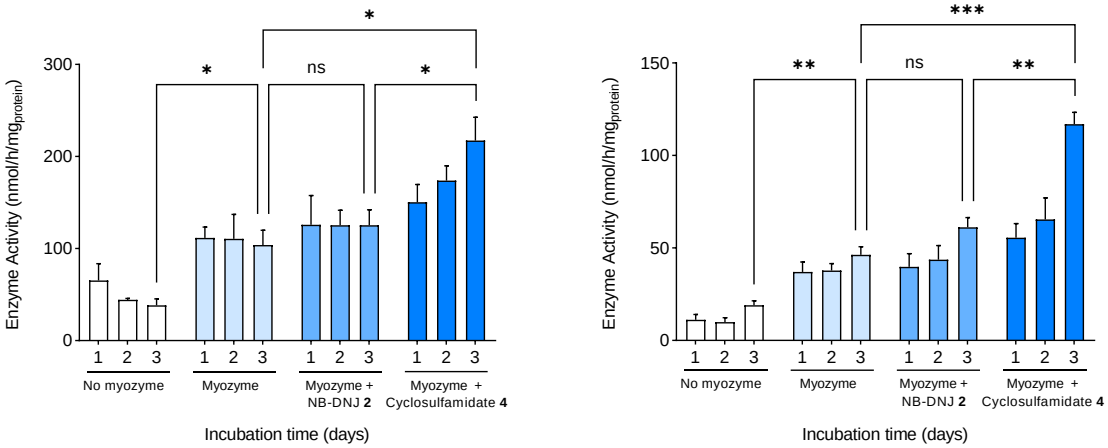


**Figure 2.8.** GAA activity in lysates of cultured Pompe disease fibroblasts treated with **2** or **4** in combination with or without Myozyme. Fibroblasts from adult Pompe disease patient, and incubated for 1-3 days with Myozyme (alglucosidase alpha, 10 nM) in combination with or without 20 μM NB-DNJ **2** or cyclosulfamidate **4**. Experiments were performed in biological triplicates and technical triplicates, both graphs performed at two different cell passage numbers. Data are depicted as mean ± SD and analysed using a Two-Way ANOVA with Tuckey's multiple comparisons test. *$p < 0.05$.

The transport and processing of endocytosed lysosomal rhGAA in cultured human skin fibroblasts has been well documented, and differences in apparent molecular mass between the exogenous rhGAA (105 KDa) and corresponding lysosomal forms (70 and 76 KDa) were assigned to differences in glycosylation.[34,35] Notably, an increase of rhGAA's 70 and 76 KDa isoforms was detected over time, which indicated that cyclosulfamidate **4** may assist in the transport of rhGAA to lysosomes in Pompe fibroblasts as well (Figure 2.9). The rhGAA stabilization as revealed by the enhanced turnover of 4-MU glucoside (Figure 2.8) correlated well with the enhanced labelling intensity of rhGAA with α-glucosidase Cy5 ABP **34** (Figure 2.9). Of note, the stabilization effect of cyclosulfamidate **4** was superior to the one observed with NB-DNJ **2** also by ABPP analysis.

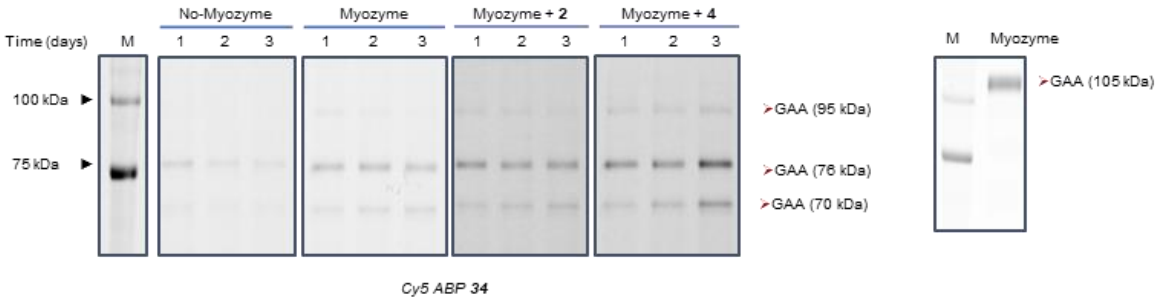


**Figure 2.9.** GAA activity in lysates of cultured Pompe disease fibroblasts from panel B visualised with activity-based probe (ABP) **34**. Lysates (3 μg per well) were first incubated with ABP **35** (Bodipy green fluorescence) to block GBA activity and GAA (three isoforms) was then visualised by incubation with ABP **34** (Cy5 fluorescence.

To analyse rhGAA stabilization *in vivo,* an enzyme stabilization assay in an easily accessible *in vivo* animal system was developed. For this, wild-type zebrafish of 2 days postfertilization (2 dpf) were injected intravenously into the sinus venous/duct of Cuvier with Myozyme (34 pmol) or a combination of Myozyme (34 pmol) and either NB-DNJ **2** or cyclosulfamidate **4** at different molar ratios (1:0.2, 1:1, 1:4 or 1:10 Myozyme:chaperone). After 5 dpf, zebrafish embryos were homogenized, and α-glucosidase activity was measured using the 4-MU-D-glucopyranoside fluorogenic substrate. Zebrafish larvae injected with Myozyme showed a significant increase in GAA activity (7.5 %) compared to nontreated controls. Zebrafish treated with Myozyme in combination with cyclosulfamidate **4** showed a significantly increased GAA activity (± 25% at 1:4 ratio) at 5 dpf compared to the zebrafish injected with only Myozyme. (Figure 2.10). This indicated the ability of sulfamidate **4** to stabilize recombinant enzyme *in vivo* and that this stabilization was slightly more efficient than the one observed with NB-DNJ **2**. High concentrations of reversible inhibitors **2** and **4** (1:10 ratio) showed a small decrease in GAA activity, which indicated that a high concentration of ligand might inhibit Myozyme as well as endogenous GAA. Of note, this experiment was limited by the amount of volume (2 nL) and concentration of the rhGAA stock that could be injected in the 2 dpf zebrafish.

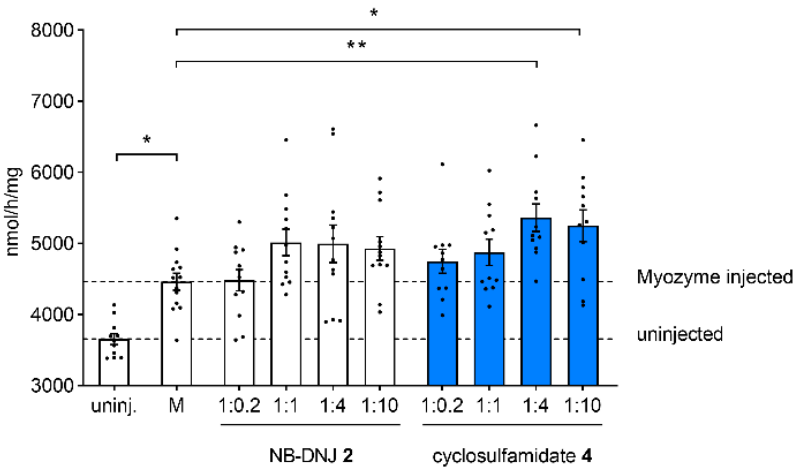


**Figure 2.10.** GAA activity in homogenates of 5 days post-fertilization (dpf) zebrafish injected with Myozyme alone or in combination with **2** or **4**. Myozyme (34 pmol in 1 nL) or Myozyme combined with NBD-DNJ **2** or sulfamidate **4** (molar ratios of 1:0.2, 1:1, 1:4 and 1:10 Myozyme:inhibitor) was injected into the sinus venous/duct of Cuvier of 2 dpf wildtype zebrafish. GAA activity was measured in homogenates of 5 dpf zebrafish larvae. Injections were performed at three independent times and at least three biological replicates were measured per injection/zebrafish. Uninjected zebrafish, n = 11; Myzoyme injected (M), n = 13; M + 6.8 pmol **2**, n = 12; M + 34 pmol **2**, n = 12; M + 136 pmol **2**, n = 12; M + 340 pmol **2**, n = 12; M + 6.8 pmol **4**, n = 11; M + 34 pmol **4**, n = 11; M + 136 pmol **4**, n = 11; M + 340 pmol **4**, n = 11 Data are depicted as mean ± SD and analysed using a One-Way ANOVA with Dunnett's multiple comparisons test with Myozyme alone as control column. *$p < 0.05$.

## 2.3 Conclusion

In conclusion, rationally designed 1,6-*epi*-cyclophellitol cyclosulfamidate **4** was developed as a selective reversible α-glucosidase ligand able to bind through $^4C_1$ conformational Michaelis complex mimicry. Kinetic and crystallographic studies of rhGAA demonstrated that the position of the endocyclic nitrogen dictated the reactivity of these cyclic sulfamidates, and whereas cyclosulfamidate **6** reacted covalently, sulfamidate **4** bound in a competitive manner, providing a new chemical space for potential α-glucosidase stabilizers. By reversible occupancy of the enzyme active, cyclosulfamidate **4** stabilized rhGAA and prevented its degradation *in vitro*, in cell medium and plasma from Pompe patients, *in situ* in Pompe fibroblasts, and *in vivo* zebrafish larvae, facilitating the enzyme transport towards the lysosome. To conclude, cyclosulfamidate **4** presented a superior stabilization and selectivity profile compared to NB-DNJ **2**, the benchmark compound in clinical combination ERT/PCT trials for the treatment of Pompe disease.

## 2.4 Acknowledgements

Rebecca E. Katzy, Dr. Chi-Lin Kuo, and Dr. Lindsey T. Lelieveld are kindly acknowledge for the inhibition kinetics and the enzyme stabilization experiments described in this thesis and their valuable discussions. Similarly, Dr. Liang Wu, Dr. Véronique Roig-Zamboni, Dr. Gerling Sulzenbacher and Prof. Gideon J. Davies are kindly acknowledge for the crystallographic studies in human and bacterial α-glucosidases and their valuable discussion.

## 2.5 Experimental methods

### 2.5.1 Biochemical experiments

#### *In vitro* apparent $IC_{50}$ experiments

To determine *in vitro* apparent $IC_{50}$ values, 40 µL of enzyme-mixture was pre-incubated with 40 µL of inhibitor **4** (0-250 µM), **6** (0-100 µM) and **2** (0-100 µM) and **3** (0-150 nM) for 30 min in the following buffers: GAA in 150 mM McIlvaine buffer pH 4.0, 0.1% bovine serum albumin (BSA) (w/v) and 2% DMSO (v/v). GANAB in 150 mM McIlvaine buffer pH 7.0, 0.1% BSA (w/v) and 2% DMSO (v/v). GBA1 in 150 mM McIlvaine buffer pH 5.2, 0.2% Taurocholate (w/v), 0.1% Triton X-100 (v/v), 0.1% BSA (w/v), 2% DMSO (v/v). GBA2 in 150 mM McIlvaine pH 5.8, 0.1% BSA (w/v).

After preincubation, 25 µL of E+I mixture was added to a 96 wells plate and 100 µL substrate solution in the appropriate buffer was subsequently added. GAA activity was measured using final concentrations of 47 nM enzyme (Myozyme) and 3.0 mM 4-MU-α-D-glucopyranoside, for 30 minutes at 37 ℃. GANAB activity was measured using wt fibroblasts and 2.4 mM 4-MU-α-D-glucopyranoside, for 2 h at 37 ℃. GBA1 activity was measured using final concentrations of 0.7 nM enzyme (Cerezyme) and 3.0 mM 4-methylumbeliferone(4-MU)-β-D-glucopyranoside, for 30 min at 37 ℃. GBA2 residual activity was measured using cellular homogenates of HEK293T over-expressing GBA2 pre-incubated for 30 min with a GBA1 inhibitor[36], and further incubation with 3.0 mM 4-methylumbeliferone(4MU)-β-D-glucopyranoside for 1h at 37℃.

Finally, all enzyme reactions were quenched with 1M NaOH-Glycine (pH 10.3) and hydrolysed 4-MU fluorescence measured with a LS55 fluorescence spectrophotometer (Perkin Elmer; $\lambda_{EX}$ 366 nm, $\lambda_{EM}$ 445 nm). Values plotted for [I] are those in the final reaction mixture, containing E + I + S. *In vitro* $IC_{50}$ values were determined from technical triplicate.

#### Competitive activity-based protein profiling (cABPP) in mouse intestine homogenates

Duodenum from wild type mice were isolated according to guidelines approved by the ethical committee of Leiden University (DEC#13191). Homogenization was performed in KPi buffer (25 mM $K_2HO_4$/$KH_2PO_4$, 0.1% (v/v) Triton X-100, protease inhibitor cocktail (EDTA-free, Roche)) with silent crusher S equipped with Typ 7 F/S head (30,000 rpm, 3 cycles of 7 sec) on ice, at a ratio of 4 µL buffer per 1 mg tissue. Protein concentration was determined with BCA Protein Assay Kit (Thermo Fisher). For cABPP, duodenum homogenates were firstly equilibrated for 5 min on ice in 4 volumes of McIlvaine buffer at pH 4.0, 6.0, or 7.0. Samples (10 µL, 60 µg total protein) were then subjected to inhibitor incubation (**2** or **4**, various concentrations, 2.5 µL in 2.5% (v/v) DMSO/$H_2O$) for 30 min at 37°C, before ABP labelling (2.5 µL) for 15 min at 37°C with JJB383 **34** (3 µM in 3 % (v/v) DMSO/McIlvaine buffer at pH 4.0 (SI + MGAM) or pH 7.0 (SI + GANAB)), MDW933 **35** (6 µM in 3 % (v/v) DMSO/McIlvaine buffer at pH 6.0) for LPH phlorizin hydrolase pocket, or TB652 **36** (6 µM in 3 % (v/v) DMSO/McIlvaine buffer at pH 6.0) for LPH lactase pocket (see Figure S2.1 for chemical structures). Samples were subsequently denatured and subjected to SDS-PAGE and fluorescent scanning according to previously described methods.

#### Time-dependent inhibition of GAA

To study the type of inhibition 20 µL rhGAA (Myozyme, 47 nM in 150mM McIlvaine buffer pH 4.0, 0.1% BSA) was pre-incubated for, 15, 30, 45, 60, 120, 180, 240 minutes at 37℃ with 20 µL of inhibitors **4** (66 µM in 150 mM McIlvaine buffer pH 4.0, 0.1% BSA, 2% DMSO) or **6** (5.1 µM in 150 mM McIlvaine buffer pH 4.0, 0.1 % BSA, 2% DMSO). After preincubation, 25 µL of enzyme + inhibitor mixture was added to a 96 well plate and 100 µL substrate solution (3.0 mM 4-MU-α-D-glucopyranoside) in the previous buffer was added and incubated for 30 minutes at 37 ℃. Finally, enzyme reactions were quenched with 1M NaOH-Glycine (pH 10.3) and liberated 4-MU fluorescence was measured with a LS55 fluorescence spectrophotometer (Perkin Elmer; $\lambda_{EX}$ 366 nm, $\lambda_{EM}$ 445 nm). Time was plotted against residual enzyme activity. Time-dependent GAA inhibition assays were performed in technical triplicate.

**Kinetic studies**

Kinetic paramaters for inhibition of GAA were determined using a fluorogenic substrate assay involving the simultaneous exposure of enzyme substrates and inhibitors and various concentrations. During the enzymatic reaction, the concentration of enzyme (rhGAA) was 47 nM in 150 mM McIlvaine buffer pH 4.0, 0.1% BSA and the concentration of substrate was 3 mM. For each inhibitor triplicate sets of 2 mL Eppendorf tubes were prepared. For irreversible inhibitor kinetics, 8.13 µL inhibitor at various concentrations (diluted in DMSO 200x reaction concentration) was added to an Eppendorf tube followed by 154.4 µL McIlvaine buffer (150 mM McIlvaine buffer pH 4.0) and 1300 µL substrate mixture (2.4 mM 4-MU-α-D-glucopyranoside, pH 4.0, 0.1% (w/v) BSA). The 2 mL eppendorf tubes were pre-heated for 10 min in a thermal shaker at 37 ℃. For each inhibitor concentration the enzyme was prepared by diluting with McIllvaine buffer in an Eppendorf tube to a volume of 1250 µL. A negative control (enzyme blanc) was prepared in a separate 2 mL Eppendorf tube by using denatured enzyme (rhGAA) which was pre-boiled (98 ℃ for 5 min). Both enzyme and blanc were pre-warmed on a thermoshaker at 37 ℃ for 10 min. Prior to the reaction a 96-black well plate was prepared with 200 µL stop buffer (1M NaOH-Glycine, pH 10.3) per well. The t=0 samples were prepared by filling the first columns with 12.5 µL enzyme (or enzyme blanc in the last column) and 112.6 of each of the substrate-inhibitor mix. To start the reaction 137.6 µL aliquots of pre-warmed enzyme to each of the pre-warmed 2 mL Eppendorf tubes containing the substrate-inhibitor mixture with an interval of 10 seconds. To ensure proper mixing of the separate components during addition of the enzyme aliquots the 2 mL Eppendorf tubes were continuously shaken in a thermoshaker at 37 ℃. At t = 4 min, 6 min, 8 min, 10 min, duplicates aliquots of 125 µL from each of the reaction tubes were transferred to the 96-well plate that contained stop buffer with a 10 second interval between samples. The plate was shortly vortexed after which 4-MU fluorescence was measured immediately. When reversible inhibition was observed similar experimental conditions were used with relevant inhibitor concentration (100 µM) and a range of substrate (4-MU-α-D-glucopyranoside, pH 4.0, 0.1% (w/v) BSA) concentrations. The observed pseudo first order inactivation rate ($k_{obs}$) was calculated for each concentration of each inhibitor by fitting the data with the one-phase exponential association function: 4-MU fluorescence = A*(1-e^( $k_{obs}$*t)) using GraphPad Prism. The obtained $k_{obs}$ values for each concentration of each inhibitor were then plotted against the inhibitor concentration, the resulting plots were plotted using a linear function which gives combined apparent inhibition parameter $k_{inact}/K'_I$ as the slope. $k_{inact}/K_I$ was derived from $k_{inact}/K'_I$ by correcting for the presence of competing 4-MU-α-D-glucopyranoside substrate using the relationship: $K'_I = K_I(1+[S]/K_M)$. $K_I$ values for reversible inhibition were determined by linear mixed-inhibition kinetics.

**Thermo-stability assays (TSAs)**

**Thermofluor methods for TSA of bacterial α-Glucosidase *Cj*Agd31B**. Thermal shift assay (TSA) reactions were assembled to a final volume of 25 µL in 50 mM Sodium Citrate pH 6.5 buffer, containing 2 µM *Cj*Agd31B, 2x Sypro Orange dye (Sigma, 5000x stock concentration), and 0–1000 µM inhibitor (Figure S2.3). All conditions were carried out in triplicate. Reactions were run on a Stratagene Mx3005P qPCR instrument (Agilent), across a temperature range of 25–95 ºC, linearly incremented at a rate of 1ºC per 30 seconds. Sypro Orange fluorescence was measured every 30 seconds, using wavelengths of $\lambda_{ex}$ = 517 nm and $\lambda_{em}$ = 585 nm. Fluorescence measurements *vs* temperature for each TSA reaction were fitted to a 5-parameter sigmoidal function ($y = T_{min} + (T_{max} - T_{min})/(1 + e(A – x)B)^C$ with melting temperature ($T_M$) determined as the midpoint of the plotted curves. Calculated $T_M$ values were used to generate a plot of $T_M$ *vs* inhibitor concentration for each inhibitor, which was subsequently fitted to a 4 parameter logistic function ($y = T_{M\_min} + (T_{M\_max} - T_{M\_min})/(1 + (x/EC_{50})^B$) to give the $EC_{50}$ and maximal $\Delta T_M$ of thermal stabilization for each inhibitor.

**Stability of Myozyme determined by the Tycho NT.6**. In a final volume of 30 µL, Myozyme (1 µM) was incubated with 0 µM – 20 µM of compound in 50 mM Sodium Citrate buffer pH 6.5. Samples were incubated at RT for two hours, after which each sample was measured in triplicate on the Tycho NT.6. Inflection points (defined as the maximum of the first derivative) as determined by the Tycho NT.6 were plotted against the compound concentration and the $EC_{50}$ and maximum shift in inflection temperature ($\Delta T_i$) were calculated using GraphPad Prism version 9.

***In vitro* stabilization of α-glucosidase A in fibroblasts**

Adult Pompe fibroblasts, cultured in DMEM/F12 + 10 % FCS + P/S at 5 % $CO_2$, were seeded during split (1:4) in 24 well plates. Medium was refreshed weekly, and experiments were started two weeks after the 1:4 passage date. Recombinant human GAA (rhGAA, Myozyme) was diluted to 10 nM in DMEM/F12 and compounds in DMSO were added to final concentration of 20 µM, with a final DMSO concentration of 0.5 %. After incubation, cells were washed three times with PBS and scraped in 30 µL lysis buffer (20 mM KPi pH 6.5 supplemented with 0.1 % Triton X-100 and protease inhibitor, no EDTA). After 30 min incubation on ice, lysates were stored at -80 °C until use. To examine the stability of Myozyme under experimental conditions, samples of the used medium with Myozyme and compounds were also incubated at 37 °C, 5 % $CO_2$, and frozen at -80 °C after collection.

Protein concentrations were determined using the Pierce BCA kit, with lysates diluted 3x. Specific GAA activity was determined using 3.0 mM 4-MU-α-D-glucopyranoside substrate in GAA buffer (150 mM McIlvaine buffer pH 4.0 with 0.1 % BSA) with 0.1 % DMSO. In triplicate, 2 µL lysate was diluted with 23 µL GSS buffer and incubated with 100 µL substrate for 4 hours at 37 °C. The reaction was quenched with 200 µL 1 M glycine-NaOH pH 10.3. Free 4-MU fluorescence was measured on an LS55 fluorescence spectrophotometer (Perkin Elmer; $\lambda_{EX}$ 366 nm, $\lambda_{EM}$ 445 nm).

Lysates were diluted with KPi buffer to 3 µg per well, keeping the total volume lower than 7 µL. McIlvaine buffer (150 mM, pH 4.0) was added to 12 µL. In sequence, the ABPs (200 nM ABP **34** followed by 500 nM ABP **33**) were added and each incubated for 30 min at 37 °C. After incubation the reaction was stopped by adding Laemmli sample buffer and incubation at 95 °C for 5 min. Samples were run on a 7.5 % SDS-PAGE gel and scanned using a Typhoon variable mode imager (GE Healthcare Bio-Science Corp., Piscataway, NJ).

***In vitro* stabilization of rhGAA in plasma**

Recombinant human GAA (rhGAA, Myozyme) was diluted to 10 nM in plasma from healthy individuals (Sanquin, The Netherlands) or Plasma from adult Pompe patients kindly donated by the biobank from patients affected by ALS, neuromuscular and lysosomal diseases (University Hospital of Udine, Italy): patient 1 with genotype: p.L355P; p. R672W under ERT (last infusion 11 days before sampling) and patient 2 with genotype: c.-32-13T>G; p.N403K under no treatment. DMSO or compounds in DMSO were added to final concentration of 20 µM, with a final DMSO concentration of 0.5 %. Samples were taken every hour and kept on ice or frozen at -80 °C until α-glucosidase activity analysis. Specific GAA activity was determined as described above, with an incubation time of 2 hours.

***In vivo* stabilization of rhGAA in zebrafish embryo**

Zebrafish husbandry and embryo injections.

Zebrafish (Strain AB/TL) were housed at Leiden University, The Netherlands, and maintained and handled in compliance with the directives of the local animal welfare committee (Instantie voor Dierwelzijn, IvD, Leiden) and guidelines specified by the EU animal Protection Directive 2010/63/EU. Wildtype embryos were acquired by natural spawning at the onset of the light period and embryos were raised in egg water (60 µg/L Instant Ocean Sera Marin™ aquarium salts (Sera; Heinsberg, Germany). Injection mixtures were prepared by combining Myozyme (40 µM) with DMSO, NBD-DNJ **2** or sulfamidate **4**, in different molar ratios, in 0.5% Phenol Red solution in DPBS (Sigma). Final mixtures contained 34 µM Myozyme without inhibitor or with 6.8 µM, 34 µM, 136 µM or 340 µM inhibitor for 1:0.2, 1:1, 1:4 or 1:10 molar ratio of Myozyme:inhibitor respectively, and 0.95% (v/v) DMSO. Two day old zebrafish (52-56 hours post-fertilization) were anesthetized in 0.01% tricaine and 1 nL of the Myozyme mixture (with or without inhibitor) was injected into the sinus venous/duct of Cuvier. After injection, the zebrafish larvae were washed twice with egg water and raised to 5 dpf at 28.5 °C. Pools of five 5 dpf zebrafish larvae were harvested, homogenized in 100 µL of KPi Buffer and 12.5 µL of this lysate was used to measure GAA activity as described above with 4-MU-α-glucoside as fluorogenic substrate (Figure 5). Injections were performed two independent times and at least three biological replicates were measured per injection.

**Crystallographic data collection and refinement of recombinant human acid α-glucosidase (rhGAA, Myozyme®)**

The enzyme source were residual amounts of the infusions of Myozyme® (Sanofi Genzyme, Cambridge, MA) administrated for the treatment of Pompe patients at the Department of Translational Medical Sciences, Federico II University, Naples, Italy. Sample conditioning and crystallization were performed as described previously.[22] Complex crystals were obtained by adding small amounts of powder of cyclosulfamidates **4** and **6,** respectively, to the crystallization droplets, followed by incubation for ~1 h. Crystals were cryo-protected with reservoir solution supplemented with 15% (v/v) glycerol prior flash cooling in liquid $N_2$. Diffraction data were collected at beamline Proxima2 of the Synchrotron Soleil, Gif-sur-Yvette, France. Data were integrated and scaled with XDS[37] and the CCP4 software suite.[38] The structures were solved by difference Fourier synthesis with REFMAC5[39] using the native structure of rhGAA (PDB entry 5NN3) as starting model. Ligand coordinates were generated with jLigand[40] and the models were adjusted with subsequent rounds of Refmac5[39] and Coot[41], respectively. Indices for the $R_{free}$ cross-validation data sets were taken over from PDB entry 5NN4. Model quality was assessed with internal modules of Coot[41] and with the Molprobity server.[42] Figures were generated with Pymol (The PyMOL Molecular Graphics System, Version 2.3.5, Schrödinger, LLC.)

**Crystallographic data collection and refinement of bacterial α-glucosidase *Cj*Agd31B**

*Cj*Agd31B expression, purification and crystallization was carried out as previously described.[32] Ligand complexes were obtained by soaking *Cj*Agd31B crystals in cryoprotectant solution (0.1 M HEPES pH 7.0, 2 M $Li_2SO_4$, 2% PEG400) supplemented with 5 mM ligand for 2 h, before harvesting and flash cooling in liquid $N_2$ for data collection.

Data were collected at beamline I04 of the Diamond light source, UK. Reflections were autoprocessed using the xia2 pipeline[43] of the CCP4 software suite (Table S1). Complexes were solved by directly refining against an unliganded *Cj*Agd31B structure (PDB accession 4B9Y) using REFMAC5[44], then further improved through subsequent rounds of manual model building and refinement using Coot[45] and REFMAC5 respectively. All ligand coordinates were built using jLigand.[40] Figures were generated using Pymol.

### 2.5.2 Chemical synthesis

**General experimental details**

All reagents were of experimental grade and were used without further purification unless stated otherwise. Dichloromethane (DCM) and tetrahydrofuran (THF) were stored over 3 Å molecular sieves and *N,N*-dimethylformamide (DMF) was stored over 4 Å molecular sieves, which were dried *in vacuo* before use. All reactions were performed under an $N_2$ atmosphere unless stated otherwise. Reactions were monitored by analytical thin layer chromatography (TLC) using Merck aluminum sheets pre-coated with silica gel 60 with detection by UV-absorption (254 nm) and by spraying with a solution of $(NH_4)_6Mo_7O_{24}\cdot H_2O$ (25 g/L) and $(NH_4)_4Ce(SO_4)_4\cdot H_2O$ (10 g/mL) in 10% sulfuric acid followed by charring at ~150 ℃ or by spraying with an aqueous solution of $KMnO_4$ (7%) and $K_2CO_3$ (2%) followed by charring at ~150 ℃. Column chromatography was performed manually using either Baker or Screening Device silica gel 60 (0.04-0.063 mm) or a Biotage Isolera™ flash purification system using silica gel cartridges (Screening Device SilicaSep HP, particle size 15-40 μm, 60A) in the indicated solvents. $^1$H-NMR and $^{13}$C-NMR spectra were recorded on Bruker AV-500 (500/126 MHz), and Bruker AV-400 (400/101 MHz) spectrometer in the given solvent. Chemical shifts are given in ppm ($\delta$) relative to the chloroform, methanol or dimethylsulfoxide residual solvent peak or tetramethylsilane (TMS) as internal standard. All given $^{13}$C-NMR spectra are proton decoupled. The following abbreviations are used to describe peak patterns when appropriate: s (singlet), d (doublet), t (triplet), q (quartet), m (multiplet), Ar (aromatic), $C_q$ (quarternary carbon). 2D NMR experiments (HSQC, COSY) were carried out to assign protons and carbons of the new structures and numbering and assignation follows the general numbering shown in Figure 2.9. High-resolution mass spectra (HRMS) of compounds were recorded with an LTQ Orbitrap (Thermo Finnigan) equipped with an electronspray ion source in positive mode (source voltage 3.5 kV, sheath gas flow 10 mL/min, capillary temperature 250 ℃) with resolution R = 60000 at m/z (400 mass range m/z = 150 – 2000) and dioctyl phthalate (m/z = 391.28428) as a lock mass. The high-resolution mass spectrometer was calibrated prior to measurements with a calibration mixture (Thermo Finnigan). Optical rotations were measured on a Anton Paar MCP automatic polarimeter (Sodium D-line, λ = 589 nm). LC-MS analysis was performed on a LCQ Advantage Max (Thermo Finnigan) ion-trap spectrometer (ESI+) coupled to a Surveyor HPLC system (Thermo Finnigan) equipped with a C18 column (Gemini, 4.6 mm x 50 mm, 3 μM particle size, Phenomenex) equipped with buffers A: $H_2O$, B: acetonitrile (MeCN) or an Agilent technologies 1260 infinity LC-MS with a 6120 Quadrupole MS system equipped with buffers A: $H_2O$, B: acetonitrile (MeCN) and C: 100 mM $NH_4OAc$. IR spectra were recorded on a Shimadzu FTIR-8300 and are reported in cm$^{-1}$. α-Glucosidase ABP JJB 383 **34**[46], selective GBA β-glucosidase ABP MDW 933 **35**[47], α-galactosidase ABP TB652 **36**[48] and inhibitor ME656 **37**[36] were synthesized following previously described procedures.

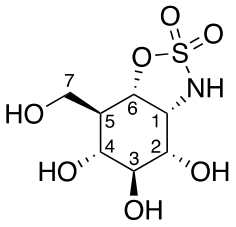


**4**

**Figure 2.11** General numbering.

**Synthesis and characterization data of 4 and 5**

**(1*R*,2*S*,3*S*,4*S*,5*R*,6*S*)-2-Azido-3,4,5-tris(benzyloxy)-6-((benzyloxy)methyl)cyclohexan-1-ol (10) and (1*R*,2*S*,3*R*,4*R*,5*S*,6*S*)-2-azido-4,5,6-tris(benzyloxy)-3-((benzyloxy)methyl) cyclohexan-1-ol (11):** Epoxide **9**[49] (0.57 g, 1.06 mmol) was dissolved in anhydrous DMF (22.3 mL) and $NaN_3$ (1.38 g, 21.2 mmol, 20 eq) was added to the mixture. The reaction was stirred overnight at 80 °C. The reaction mixture was allowed to cool down to rt, diluted with $H_2O$ and the aqueous phase was extracted with $Et_2O$ (2x). The combined organic layers were washed with $H_2O$ and brine, dried over $MgSO_4$, filtered and concentrated *in vacuo*. The crude reaction mixture was purified by silica gel chromatography (Pentane/EtOAc 90:10 → 70:30) to obtain **10** (0.23 g, 0.4 mmol, 38%) and **19** (0.21 g, 0.36 mmol, 34%).

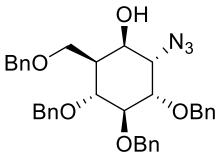


**Azide (10):** $^1$H NMR (500 MHz, $CDCl_3$) $\delta$ 7.39 – 7.35 (m, 2H, $CH_{Ar}$), 7.35 – 7.24 (m, 16H, $CH_{Ar}$), 7.21 – 7.18 (m, 2H, $CH_{Ar}$), 4.95 (d, $J$ = 10.8 Hz, 1H, CH*H*Ph), 4.93 (d, $J$ = 10.8 Hz, 1H, CH*H*Ph), 4.82 (d, $J$ = 10.7 Hz, 1H, CH*H*Ph), 4.77 (d, $J$ = 11.5 Hz, 1H, CH*H*Ph), 4.73 (d, $J$ = 11.5 Hz, 1H, CH*H*Ph), 4.50 (d, $J$ = 10.9 Hz, 1H, CH*H*Ph), 4.46 (d, $J$ = 11.7 Hz, 1H, CH*H*Ph), 4.39 (d, $J$ = 11.7 Hz, 1H, CH*H*Ph), 4.11 – 4.03 (m, 4H, CH*H*Ph, C-1, C-2, C-7), 3.97 – 3.91 (m, 2H, CH-4, CH-6), 3.85 (t, $J$ = 9.3 Hz, 1H, CH-3), 3.67 (dd, $J$ = 9.2, 2.4 Hz, 1H, CH-7), 1.91 (dq, $J$ = 11.3, 2.5 Hz, 1H, CH-5), 1.57 (s, 1H, OH). $^{13}$C NMR (126 MHz, $CDCl_3$) $\delta$ 138.9, 138.7, 138.2, 137.1 ($4C_q$), 128.8, 128.6, 128.5, 128.5, 128.3, 128.1, 128.0, 127.99, 127.9, 127.9, 127.8, 127.7 ($12CH_{Ar}$), 84.2 (C-3), 80.3 (C-2), 76.6 (C-4), 75.9, 75.7, 73.9, 73.5 ($4CH_2Ph$), 72.8 (C-1), 70.2 (C-7), 62.7 (C-6), 41.2 (C-5). HRMS: calcd. for $[C_{37}H_{35}N_3NaO_5]^+$ 602.26254; found 602.26228, calcd. for $[C_{37}H_{39}N_4O_5]^+$ 597.30715; found 597.30691.

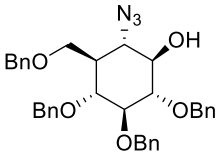


**Azide (19):** $^1$H NMR (400 MHz, $CDCl_3$) $\delta$ 7.39 – 7.24 (m, 18H, $CH_{Ar}$), 7.19 (dd, $J$ = 7.4, 2.0 Hz, 2H, $CH_{Ar}$), 4.96 (d, $J$ = 11.3 Hz, 1H, CH*H*Ph), 4.87 (d, $J$ = 11.1 Hz, 3H, CH*H*Ph), 4.73 (d, $J$ = 11.2 Hz, 1H, CH*H*Ph), 4.54 (d, $J$ = 10.7 Hz, 1H, CH*H*Ph), 4.49 (d, $J$ = 11.8 Hz, 1H, CH*H*Ph), 4.43 (d, $J$ = 11.7 Hz, 1H, CH*H*Ph), 3.82 – 3.73 (m, 1H, CH*H*Ph), 3.73 – 3.68 (m, 1H, CH*H*Ph), 3.66 (dd, $J$ = 9.2, 2.4 Hz, 1H, CH-7), 3.61 – 3.51 (m, 2H, CH-4, CH-7), 3.48 (d, $J$ = 10.8 Hz, 1H, CH-1), 3.37 (t, $J$ = 9.2 Hz, 1H, CH-3), 2.54 (d, $J$ = 2.1 Hz, 1H, CH-6)), 1.56 (s, 1H, OH), 1.49 (tt, $J$ = 11.1, 2.3 Hz, 1H, CH-5). $^{13}$C NMR (101 MHz, $CDCl_3$) $\delta$ 138.5, 138.4, 138.3, 138.2 ($4C_q$), 128.8, 128.6, 128.59, 128.5, 128.2, 128.1, 128.0, 127.97, 127.92, 127.83 ($10CH_{Ar}$), 85.63 (C-3), 83.09 (C-2), 77.82 (C-4), 76.08 (C-1), 75.85, 75.76, 75.68, 73.28 ($4CH_2Ph$), 64.80 (C-7), 61.45 (C-6), 44.76 (C-5). HRMS: calcd. for $[C_{37}H_{35}N_3NaO_5]^+$ 602.26254; found 602.26238, calcd. for $[C_{37}H_{39}N_4O_5]^+$ 597.30715; found 597.30703.

**(1*R*,2*S*,3*R*,4*R*,5*S*,6*S*)-2-Amino-4,5,6-tris(benzyloxy)-3-((benzyloxy)methyl) cyclohexan-1-ol (11):** Azide **10** (0.23 g, 0.4 mmol) was dissolved in anhydrous THF (10 mL) and the solution was purged with $N_2$. $PtO_2$ (36 mg, 0.16 mmol, 0.4 eq) was added and the reaction mixture was purged again with $N_2$. The reaction was then stirred under $H_2$ atmosphere, for 4 h at rt. The reaction was flushed with $N_2$, filtered over a celite plug and concentrated *in vacuo*. The crude mixture was purified by silica gel column chromatography (Pentane/Acetone 100:1 → 40:60) to afford pure **11** (0.22 g, 0.39 mmol, 98 %).

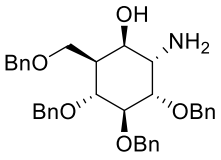


$^1$H NMR (400 MHz, $CDCl_3$) $\delta$ 7.40 – 7.19 (m, 20H, CH Ar), 4.95 (d, $J$ = 10.2 Hz, 2H, CH*H*Ph), 4.83 (d, $J$ = 10.8 Hz, 1H, CH*H*Ph), 4.73 (d, $J$ = 11.5 Hz, 1H, CH*H*Ph), 4.69 (d, $J$ = 11.5 Hz, 1H, CH*H*Ph), 4.55 (d, $J$ = 11.0 Hz, 1H, CH*H*Ph), 4.51 (d, $J$ = 11.7 Hz, 1H, CH*H*Ph), 4.44 (d, $J$ = 11.7 Hz, 1H, CH*H*Ph), 4.13 (dd, $J$ = 9.1, 3.1 Hz, 1H, CH-7a), 4.05 (dd, $J$ = 3.5, 2.1 Hz, 1H, CH-2), 4.04 – 3.90 (m, 3H, CH-1, CH-4, CH-6), 3.73 (dd, $J$ = 9.1, 2.4 Hz, 1H, CH-7b), 3.50 (t, $J$ = 3.6 Hz, 1H, CH-3), 2.30 – 2.23 (m, 1H, CH-5). $^{13}$C NMR (101 MHz, $CDCl_3$) $\delta$ 139.2, 139.0, 138.9, 137.4 ($4C_q$ Ar), 128.7, 128.5, 128.5, 128.5, 128.4, 128.1, 128.0, 127.9, 127.9, 127.8, 127.7, 127.6, 127.5 (20CH Ar), 83.8 (C-1/C-6), 80.7 (C-1/C-6), 77.2 (C-4), 75.6, 75.5 ($2CH_2Ph$), 75.4 (C-2), 73.8, 72.7 ($2CH_2Ph$), 70.7 (C-7), 52.7 (C-3), 40.9 (C-5). HRMS: calcd. for $[C_{35}H_{40}NO_5]^+$ 554.29010; found 554.29054.

***Tert*-butyl ((1*S*,2*S*,3*S*,4*R*,5*S*,6*R*)-2,3,4-tris(benzyloxy)-5-((benzyloxy)methyl)-6-hydroxycyclohexyl) carbamate (12):** Amino alcohol **11** (120 mg, 0.21 mmol) was dissolved in anhydrous DCM (1.05 mL), and $Et_3N$ (0.15 mL, 1.06 mmol, 5 eq) and $Boc_2O$ (58 µL, 0.25 mmol, 1.2 eq) were added at 0 °C. The reaction was stirred overnight at rt. The reaction was quenched with sat. aq. $NH_4Cl$. The aqueous layer was extracted with DCM (3x). The combined organic layers were dried over MgSO4, filtered and concentrated *in vacuo*.

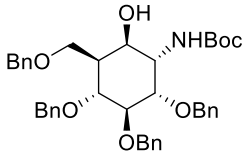

The crude product was purified by silica gel column chromatography (Pentane/EtOAc 9:1 → 7:3) to obtain **12** (113 mg, 0.17 mmol, 82%) as a colourless oil. $^1$H NMR (400 MHz, $CDCl_3$) $\delta$ 7.39 – 7.28 (m, 18H, CH Ar), 7.24 – 7.21 (m, 2H, CH Ar), 4.99 (d, $J$ = 10.8 Hz, 1H, CH*H*Ph), 4.95 (d, $J$ = 10.8 Hz, 1H, CH*H*Ph), 4.83 – 4.76 (d, 1H, CH*H*Ph)), 4.70 (d, $J$ = 11.1 Hz, 1H, CH*H*Ph)), 4.59 (d, $J$ = 11.1 Hz, 1H, CH*H*Ph), 4.52 (d, $J$ = 11.0 Hz, 1H, CH*H*Ph), 4.49 – 4.44 (m, 3H, 2CH*H*Ph, CH-6), 4.18 (m, 2H, CH-1, CH-2), 4.09 (dd, $J$ = 9.1, 3.2 Hz, 1H, CH-7a), 4.04 (dd, $J$ = 11.4, 8.9 Hz, 1H, CH-4), 3.80 (s, 1H, OH), 3.75 (dd, $J$ = 9.1, 2.5 Hz, 1H, CH-7b), 3.59 (t, $J$ = 9.1 Hz, 1H, CH-3), 1.92 (dd, $J$ = 11.4, 2.5 Hz, 1H, CH-5), 1.47 (s, 9H, $(CH_3)_3$). $^{13}$C NMR (101 MHz, $CDCl_3$) $\delta$ 156.0 (C=O), 138.9, 138.6, 138.1, 137.2 ($4C_q$ Ar), 128.6, 128.4, 128.4, 128.4, 128.1, 128.1, 127.9, 127.8, 127.8, 127.8, 127.7, 127.5 (20CH Ar), 84.3, (C-3) 78.1 (C-1), 76.4 (C-4), 75.6, 75.5, 73.7 ($3CH_2$Ph), 72.1 (C-6), 71.9 ($CH_2$Ph), 70.1 (C-7), 51.8 (C-2), 41.2 (C-5), 28.4 ($(CH_3)_3$). ). HRMS: calcd. for $[C_{40}H_{48}NO_7]^+$ 654.34253; found 654.34242.

**(1*R*,2*R*,3*R*,4*S*,5*S*,6*R*)-3,4,5-Tris(benzyloxy)-2-((benzyloxy)methyl)-6-((*tert*butoxycarbonyl)amino)cyclohexyl methanesulfonate (13):** Intermediate **12** (146 mg, 0.22 mmol) was dissolved in anhydrous $CHCl_3$ (2.20 mL) and $Et_3N$ (0.16 mL, 1.11 mmol, 5 eq), Me-imidazole (0.18 mL, 2.23 mmol, 10 eq) and MsCl (86 µL, 1.11 mmol, 5 eq) were added to the solution at 0 ℃. The reaction was stirred overnight at rt. The reaction mixture was diluted with EtOAc and the organic layer was washed with 1M HCl (3x), $H_2O$ and brine. The washed organic layer was dried over $MgSO_4$, filtered and concentrated *in vacuo*. The crude product was purified by silica gel column chromatography (Pentane/EtoAc 9:1 → 7:3) to obtain **13** (146 mg, 0.19 mmol, 91%) as a yellow oil. $^1$H NMR (500 MHz, $CDCl_3$) $\delta$ 7.34 – 7.24 (m, 18H, CH Ar), 7.18 – 7.14 (m, 2H ,CH Ar), 5.39 (m, 1H, CH-6), 4.91 (d, $J$ = 10.8 Hz, 1H, CH*H*Ph), 4.85 – 4.81 (m, 2H, CH*H*Ph, NH), 4.74 (d, $J$ = 10.8 Hz, 1H, CH*H*Ph), 4.64 (d, $J$ = 11.3 Hz, 1H, CH*H*Ph), 4.59 (d, $J$ = 11.3 Hz, 1H, CH*H*Ph), 4.46 (d, $J$ = 12.7 Hz, 3H CH*H*Ph), 4.33 (s, 1H, CH-1), 4.00 (dd, $J$ = 9.4, 4.7 Hz, 1H, CH-2), 3.78 (dd, $J$ = 9.4, 4.3 Hz, 1H, CH-7a), 3.63 (t, $J$ = 8.9 Hz, 1H, CH-3), 3.56 (t, $J$ = 9.5 Hz, 1H, CH-4), 3.50 (s, 1H, CH-7b), 2.91 (s, 3H, $CH_3$), 2.42 (t, $J$ = 8.4 Hz, 1H, CH-5), 1.44 (s, 9H, $(CH_3)_3$). $^{13}$C NMR (126 MHz, $CDCl_3$) $\delta$ 155.7 (C=O), 138.6, 138.2, 137.9, 137.6 ($4C_q$ Ar), 128.7, 128.6, 128.6, 128.4, 128.2, 128.0, 127.9, 127.9, 127.8 (CH Ar), 83.0 (C-3), 77.7 (C-6), 77.2 (C-4), 77.1 (C-2), 75.8, 75.4, 73.1, 72.4 ($4CH_2$Ph), 66.4 (C-7), 50.8 (C-1), 40.5 (C-5), 37.6 ($CH_3$), 28.4 ($(CH_3)_3$). HRMS: calcd. for $[C_{41}H_{49}NNaO_9S]^+$ 754.30202; found 754.30105, calcd. for $[C_{41}H_{53}N_2O_9S]^+$ 749.34663; found 749.34611 .

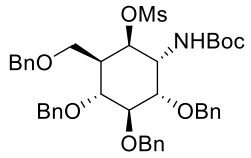


**(3a*S*,4*S*,5*S*,6*R*,7*S*,7a*S*)-4,5,6-Tris(benzyloxy)-7-((benzyloxy)methyl) hexahydrobenzo[*d*]oxazol-2(3*H*)-one (14):** Intermediate **13** (140 mg, 0.19 mmol) was dissolved in anhydrous DMF (8.7 mL) and the reaction mixture was stirred for 24 h at 120 ℃. The reaction was then cooled to rt and diluted with $H_2O$. The aqueous phase was extracted with EtOAc (3x) and the combined organic layers were washed with $H_2O$ (2x) and brine, dried over $MgSO_4$, filtered and concentrated *in vacuo*. The crude product was purified by silica gel column chromatography (Pent/EtOAc 100:1 → 50:50) to obtain **14** (70 mg, 0.12 mmol, 64%) as an orange oil. $^1$H NMR (500 MHz, $CDCl_3$) $\delta$ 7.40 – 7.27 (m, 18H, CH Ar), 7.26 – 7.22 (m, 2H, CH Ar), 5.35 (s, 1H, NH), 4.83 (d, 1H, CH*H*Ph), 4.80 (dd, $J$ = 7.1, 2.1 Hz, 1H, CH-6), 4.78 (d, $J$ = 1.2 Hz, 3H, CH*H*Ph), 4.61 (d, $J$ = 11.9 Hz, 1H, CH*H*Ph), 4.57 (d, $J$ = 10.9 Hz, 1H, CH*H*Ph), 4.50 (d, $J$ = 11.7 Hz, 1H, CH*H*Ph), 4.47 (d, $J$ = 11.7 Hz, 1H, CH*H*Ph), 4.08 (dd, $J$ = 7.4, 4.3 Hz, 1H, CH-1), 3.89 (dd, $J$ = 9.3, 2.4 Hz, 1H, CH-7a), 3.86 (dd, $J$ = 8.2, 7.3 Hz, 1H, CH-3), 3.65 (dd, $J$ = 9.3, 2.2 Hz, 1H, CH-7b), 3.60 (dd, $J$ = 7.3, 4.3 Hz, 1H, CH-2), 3.56 (dd, $J$ = 11.6, 8.2 Hz, 1H, CH-4), 2.24 – 2.17 (m, 1H, CH-5). $^{13}$C NMR (126 MHz, $CDCl_3$) $\delta$ 158.9 (C=O), 138.4, 138.3, 138.1, 137.7 ($4C_q$ Ar), 128.8, 128.6, 128.6, 128.6, 128.3, 128.1, 128.0, 128.0, 127.9, 127.8 (20CH Ar), 82.5 (C-3), 77.4 (C-2), 76.2 (C-4), 75.1, 74.8 ($2CH_2$Ph), 74.2 (C-6), 73.6, 73.5 ($2CH_2$Ph), 65.5 (C-7), 54.5 (C-1), 44.6 (C-5). HRMS: calcd. for $[C_{36}H_{41}N_2O_6]^+$ 597.29591; found 597.29570, calcd. for $[C_{36}H_{37}NNaO_6]^+$ 602.25131; found 602.25088.

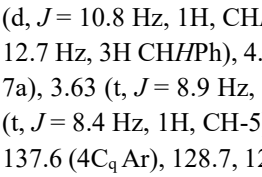


**(1*S*,2*S*,3*S*,4*S*,5*R*,6*S*)-2-Amino-3,4,5-tris(benzyloxy)-6-((benzyloxy)methyl)cyclohexan-1-ol (15):** Cyclic carbamate **14** (70 mg, 120 µmol) was dissolved in EtOH (7.2 mL) and NaOH (1M, 1.8 mL, 1.8 mmol, 15 eq) was added to the solution. The reaction was stirred at 70 ℃ for 3 h and was subsequently stirred overnight at rt. The reaction mixture was concentrated and the crude residue was diluted with $H_2O$. The aqueous phase was extracted with EtOAc (3x) and the combined organic layers were washed with $H_2O$ and brine, dried over $MgSO_4$, filtered and concentrated *in vacuo*. The crude product was purified by silica gel column chromatography (DCM/MeOH

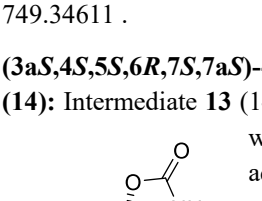

100:1→ 80:20) to obtain **15** (64 mg, 115 µmol, 96%) as a colourless oil $^1$H NMR (400 MHz, $CDCl_3$) $\delta$ 7.38 – 7.23 (m, 18H, CH Ar), 7.22 – 7.18 (m, 2H, CH Ar), 4.93 (d, $J$ = 10.7 Hz, 1H, CH*H*Ph), 4.87 (d, $J$ = 10.9 Hz, 1H, CH*H*Ph)), 4.79 (d, $J$ = 10.8 Hz, 1H, CH*H*Ph), 4.67 (s, 2H, CH*H*Ph)), 4.50 (d, $J$ = 11.6 Hz, 2H, CH*H*Ph), 4.45 (d, $J$ = 12.0 Hz, 2H, CH-6), 3.98 (t, $J$ = 9.3 Hz, 1H, CH-3), 3.85 (dd, $J$ = 9.0, 2.8 Hz, 1H, CH-7a), 3.69 – 3.60 (m, 2H, CH-6, CH-7b), 3.52 (t, $J$ = 3.7 Hz, 1H, CH-1), 3.43 (dd, $J$ = 9.6, 3.7 Hz, 1H, CH-2), 3.35 (dd, $J$ = 11.0, 9.1 Hz, 1H, CH-4), 2.32 – 2.05 (m, 4H, CH-5, $NH_2$, OH). $^{13}$C NMR (101 MHz, $CDCl_3$) $\delta$ 139.0, 138.7, 138.5, 138.1 (4$C_q$ Ar), 128.6, 128.6, 128.5, 128.5, 128.1, 128.0, 127.9, 127.8, 127.7, 127.6 (20CH Ar), 82.8 (C-3), 80.7 (C-2), 75.7, 75.2, 73.4, 72.4 (4$CH_2$Ph), 69.9 (C-6), 68.7 (C-7), 52.8 (C-1), 42.9 (C-5). HRMS: calcd. for $[C_{35}H_{40}NO_5]^+$ 554.29010; found 554.28970.

***Tert*-butyl (3a*R*,4*S*,5*S*,6*R*,7*R*,7a*S*)-4,5,6-tris(benzyloxy)-7-((benzyloxy)methyl) hexahydro-3*H*-benzo[*d*][1,2,3]oxathiazole-3-carboxylate 2,2-dioxide (16):** The amino alcohol **15** (63 mg, 0.12 mmol) was dissolved in anhydrous DCM (2.22 mL). $Et_3N$ (84 µL, 0.6 mmol, 5 eq) and $Boc_2O$ (32µL, 0.14 mmol, 1.2 eq) were added to the solution at 0 ℃ and the reaction was stirred overnight at rt. The reaction was quenched with sat. aq. $NH_4Cl$ and the aqueous phase was extracted with DCM (3x). The combined organic layers were dried over $MgSO_4$, filtered and concentrated *in vacuo*. The Boc protected intermediate was dissolved in anhydrous DCM (2.22 mL) and $Et_3N$ (0.18 mL, 1.26 mmol, 10.5 eq), imidazole (45 mg, 0.66 mmol, 5.5 eq) and $SOCl_2$ (88 µL, 1.2 mmol, 10 eq) were added at 0 ℃. The reaction was stirred at this temperature for 20 min. $H_2O$ was added to the reaction mixture and the aqueous phase was extracted with DCM (3x). The combined organic layers were dried over $MgSO_4$, filtered and concentrated *in vacuo*. The crude mixture of sulfites was dissolved in a 1:1:1 mixture of $H_2O$ (0.6 mL), EtOAc (0.6 mL) and MeCN (0.6 mL), and $NaIO_4$ (64 mg, 0.30 mmol, 2.5 eq) and $RuCl_3{\cdot}H_2O$ (6.2 mg, 30 µmol, 0.25 eq) were added at 0 ℃ and the reaction was stirred at this temperature for 1 h. The reaction was quenched with sat. aq. $Na_2S_2O_3$ and the aqueous phase was extracted with EtOAc (3x). The combined organic layers were washed with brine, dried over $MgSO_4$, filtered and concentrated *in vacuo*. The crude product was purified by silica gel column chromatography (Pentane/EtOAc 100:1 → 90:10) to obtain **16** (66 mg, 92 µmol, 77% over 3 steps) as a colourless oil. $^1$H NMR (500 MHz, $CDCl_3$) $\delta$ 7.40 – 7.23 (m, 18H, CH Ar), 7.18 – 7.15 (m, 2H, CH Ar), 5.24 (t, $J$ = 8.4, 7.3, 0.9 Hz, 1H, CH-6), 4.65 (d, $J$ = 12.2 Hz, 1H, CH*H*Ph), 4.61 (d, $J$ = 11.1 Hz, 1H, CH*H*Ph), 4.58 – 4.50 (m, 3H, CH*H*Ph), 4.48 – 4.42 (m, 2H, CH*H*Ph), 4.33 – 4.27 (m, 2H, CH*H*Ph, CH-1), 4.10 (s, 1H, CH-2), 3.87 (dd, $J$ = 9.4, 2.4 Hz, 1H, CH-7a), 3.82 (dd, $J$ = 5.6, 1.4 Hz, 1H, CH-3), 3.64 – 3.58 (m, 2H, CH-4, CH-7b), 2.73 (ddt, $J$ = 13.0, 8.8, 2.3 Hz, 1H, CH-5), 1.51 (s, 9H, $(CH_3)_3$). $^{13}$C NMR (126 MHz, $CDCl_3$) $\delta$ 148.7 (C=O), 138.2, 138.0, 137.4, 137.4 (4$C_q$ Ar), 128.7, 128.7, 128.6, 128.5, 128.5, 128.3, 128.2, 128.1, 127.9, 127.9, 127.8 (20CH Ar), 82.6 (C-3), 76.2 (C-4) , 76.1 (C-6) , 74.0 ($CH_2$Ph), 73.6 (C-2), 73.5, 73.0, 71.6 (3$CH_2$Ph), 64.9 (C-7), 56.8 (C-1), 41.1 (C-5), 28.1 ($(CH_3)_3$). HRMS: calcd. for $[C_{40}H_{45}NO_9SNa]^+$ 738.27072; found 738.27009, calcd. for $[C_{40}H_{49}N_2O_9S]^+$ 733.31533; found 733.31478.

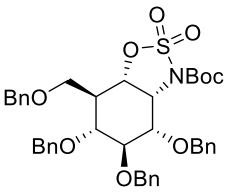

**(3a*R*,4*S*,5*S*,6*R*,7*R*,7a*S*)-4,5,6-Tris(benzyloxy)-7-((benzyloxy)methyl)hexahydro-3*H*-benzo[*d*][1,2,3]oxathiazole 2,2-dioxide (17):** Cyclosulfamidate **16** (60 mg, 84 µmol) was dissolved in anhydrous DCM (4 mL) and TFA (0.38 mL) was added to the reaction mixture. The reaction was stirred overnight at rt. The reaction mixture was diluted with $H_2O$ and the aqueous phase was extracted with DCM (3x). The combined organic layers were dried over $MgSO_4$, filtered and concentrated *in vacuo*. The crude product was purified by silica gel column chromatography (Pentane/EtOAc 95:5 → 80:20) to obtain **17** (32 mg, 52 µmol, 62%) as a colourless oil. $^1$H NMR (400 MHz, $CDCl_3$) $\delta$ 7.36 – 7.23 (m, 18H, CH Ar), 7.21 (m, 2H, CH Ar), 4.96 (dd, $J$ = 10.9, 6.5 Hz, 1H, CH-6), 4.86 (d, $J$ = 7.1 Hz, 1H, NH), 4.67 (m, $J$ = 23.4, 11.7 Hz, 4H, CH*H*Ph), 4.52 (d, $J$ = 11.5 Hz, 1H, CH*H*Ph), 4.47 (d, $J$ = 11.8 Hz, 1H, CH*H*Ph), 4.43 (d, $J$ = 11.1 Hz, 1H, CH*H*Ph), 4.38 (d, $J$ = 11.8 Hz, 1H, CH*H*Ph), 4.28 (td, $J$ = 6.8, 4.7 Hz, 1H, CH-1), 3.92 (t, 1H, CH-3), 3.80 (dd, $J$ = 6.5, 4.8 Hz, 1H, CH-2), 3.77 (dd, $J$ = 9.4, 2.1 Hz, 1H, CH-7a), 3.65 (dd, $J$ = 10.8, 5.4 Hz, 1H, CH-4), 3.59 (dd, $J$ = 9.5, 2.2 Hz, 1H, CH-7b), 2.46 (tt, $J$ = 10.8, 2.0 Hz, 1H, CH-5). $^{13}$C NMR (101 MHz, $CDCl_3$) $\delta$ 138.1, 137.8, 136.8 (4$C_q$ Ar), 128.9, 128.7, 128.6, 128.6, 128.3, 128.2, 128.0, 127.9, 127.9 (20CH Ar), 79.7 (C-6), 78.7 (C-3), 76.0 (C-4), 74.8 (C-2), 74.1, 73.9, 73.3, 73.3 (4$CH_2$Ph), 64.6 (C-7), 55.7 (C-1), 43.1 (C-5). HRMS: calcd. for $[C_{40}H_{45}NO_9SNa]^+$ 638.27072; found 638.27000, calcd. for $[C_{40}H_{49}N_2O_9S]^+$ 633.31533; found 633.31472.

**(3a*R*,4*S*,5*S*,6*R*,7*R*,7a*S*)-4,5,6-Tris(benzyloxy)-7-((benzyloxy)methyl)-3-methylhexahydro-3*H*-benzo[*d*][1,2,3]oxathiazole 2,2-dioxide (18):** $K_2CO_3$ (4.1 mg, 30 µmol 1.2 eq), TBAI (1 mg 0.1 eq) and iodomethane (3.12 µL, 49 µmol, 2 eq) were added to a solution of **17** (15 mg, 24 µmol) in anhydrous DMF (1 mL) and the reaction was stirred at rt for 5 h. The reaction mixture was diluted with EtOAc and $H_2O$ and the aqueous phase was extracted with EtOAc (3x). The combined organic layers were washed with water and brine, dried over $MgSO_4$, filtered and concentrated *in vacuo*. The crude product was purified by silica gel column chromatography (Pent/EtOAc 100:1 → 85:15) to afford **18** (10 mg, 16 µmol, 65%) as a purple oil. $^1$H NMR (500 MHz, $CDCl_3$) $\delta$ 7.37 – 7.25 (m, 18H, CH Ar), 7.21 – 7.18 (m, 2H, CH Ar), 4.88 (dd, $J$ = 10.0, 5.7 Hz, 1H, CH-6), 4.84 (d, $J$ = 11.0 Hz, 1H, CH*H*Ph), 4.76 (d, $J$ = 12.2 Hz, 3H, CH*H*Ph), 4.66 (d, $J$ = 11.7 Hz, 1H, CH*H*Ph), 4.51 (d, $J$ = 11.0 Hz, 1H, CH*H*Ph), 4.46 (d, $J$ = 11.7 Hz, 1H, CH*H*Ph), 4.40 (d, $J$ = 11.7 Hz, 1H, CH*H*Ph), 3.95 (t, $J$ = 8.3 Hz, 1H, CH-3), 3.85 – 3.81 (m, 2H, CH-1, CH-7a), 3.61 – 3.54 (m, 3H, CH-2, CH-4, CH-7b), 2.90 (s, 3H, C*H*$_3$), 2.56 (ddt, $J$ = 11.8, 9.9, 2.0 Hz, 1H, CH-5). $^{13}$C NMR (126 MHz, $CDCl_3$) $\delta$ 138.4, 138.2, 138.0, 137.4 (4$C_q$ Ar), 128.8, 128.6, 128.6, 128.3, 128.1, 128.1, 128.0, 128.0, 127.9, 127.8 (20CH Ar), 81.9 (C-3), 77.6 (C-2/C-4), 77.3 (C-6), 76.4 (C-2/C-4), 75.2, 75.1, 74.3, 73.5 (4$CH_2$Ph), 64.5 (C-7), 61.3 (C-1), 44.1 (C-5), 33.4 ($CH_3$). HRMS: calcd. for $[C_{36}H_{39}NO_7SNa]^+$ 652.23394; found 652.23382.

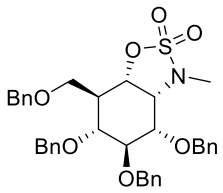


**(3A*r*,4*S*,5*S*,6*R*,7*R*,7a*S*)-4,5,6-Trihydroxy-7-(hydroxymethyl)hexahydro-3*H*-benzo[*d*][1,2,3]oxathiazole 2,2-dioxide (4):** Perbenzylated **17** (21 mg, 31 µmol) was dissolved in MeOH (1.16 mL), purged with $N_2$ and Pd/C (10 wt %, 13 mg, 12 µmol, 0.4 eq) was added and the reaction mixture was purged again with $N_2$. The reaction was then stirred overnight under $H_2$ atmosphere at rt. The reaction was flushed with $N_2$, filtered over a celite plug and concentrated *in vacuo*. The crude product was purified by silica gel column chromatography (DCM/MeOH 100:1 → 80:20) to obtain **4** (8.23 mg, 31 µmol, 99%) as a clear oil. $^1$H NMR (400 MHz, MeOD) $\delta$ 4.93 – 4.90 (1H, CH-6), 4.37 (t, $J$ = 4.8 Hz, 1H, CH-1), 4.01 (dd, $J$ = 11.2, 2.3 Hz, 1H, CH-7a), 3.70 – 3.62 (m, 2H, CH-3, CH-7b), 3.59 (dd, $J$ = 9.5, 4.3 Hz, 1H, CH-2), 3.36 – 3.33 (m, 1H, CH-4), 2.17 – 2.09 (m, 1H, CH-5). $^{13}$C NMR (101 MHz, MeOD) $\delta$ 81.7 (C-6), 74.9 (C-3), 71.0 (C-2), 69.3 (C-4), 61.0 (C-1), 57.6 (C-7), 46.6 (C-5). HRMS: calcd. for $[C_7H_{14}N_1O_7S]^+$ 256,04855; found 256,04812.

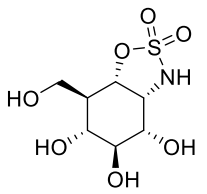


**(3a*R*,4*S*,5*S*,6*R*,7*R*,7a*S*)-4,5,6-Trihydroxy-7-(hydroxymethyl)-3-methylhexahydro-3*H*-benzo[*d*][1,2,3]oxathiazole 2,2-dioxide (5):** Perbenzylated **18** (10 mg, 16 µmol) was dissolved in a 4:1 mixture of MeOH (1 mL) and DCM (0.25 mL), purged with $N_2$ and Pd/C (10 wt %, 6.8 mg, 6.4 µmol, 0.4 eq) was added and the reaction mixture was purged again with $N_2$. The reaction was stirred overnight under $H_2$ atmosphere at rt. The reaction mixture was flushed with $N_2$, filtered over a celite plug and concentrated *in vacuo*. The crude product was purified by silica gel column chromatography (DCM/MeOH 100:1 → 80:20) to obtain **5** (2.3 mg, 8.8 µmol, 55%) as a white solid. $^1$H NMR (500 MHz, MeOD) $\delta$ 4.89 (dd, $J$ = 10.2, 5.3 Hz, 1H, CH-6), 3.98 (dd, $J$ = 11.2, 2.3 Hz, 1H, CH-7a), 3.93 (dd, $J$ = 5.3, 3.4 Hz, 1H, CH-1), 3.67 (dd, $J$ = 8.5, 2.7 Hz, 1H, CH-7b), 3.66 – 3.63 (m, 1H, CH-3), 3.59 (dd, $J$ = 9.8, 3.4 Hz, 1H, CH-2), 3.36 (dd, $J$ = 11.2, 8.7 Hz, 1H, CH-4), 2.93 (s, 3H, $CH_3$), 2.19 (tt, $J$ = 10.3, 2.5 Hz, 1H, CH-5). $^{13}$C NMR (126 MHz, MeOD) $\delta$ 79.4 (C-6), 74.7 (C-3), 72.1 (C-2), 69.7 (C-4), 64.8 (C-1), 57.5 (C-7), 47.5 (C-5), 34.5 ($CH_3$). HRMS: calcd. for $[C_8H_{16}NO_7S]^+$ 270.06420; found 270.06408.

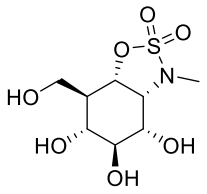

**Synthesis and characterization data of 6 and 7**

**(1*R*,2*S*,3*S*,4*S*,5*R*,6*S*)-2-Amino-3,4,5-tris(benzyloxy)-6-((benzyloxy)methyl)cyclohexan-1-ol (20):** Azide **19**

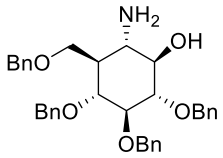


(0.21 g, 0.36 mmol) was dissolved in anhydrous THF (10 mL) and the solution was purged with $N_2$. $PtO_2$ (33 mg, 0.14 mmol, 0.4 eq) was added and the reaction mixture was purged again with $N_2$. The reaction was then stirred under $H_2$ atmosphere, for 4 h at rt. The reaction was flushed with $N_2$, filtered over a celite plug and concentrated *in vacuo*. The crude mixture was purified by silica gel column chromatography (Pentane/Acetone 100:1 → 40:60) to afford pure **20** (0.19 g, 0.35 mmol, 97 %). $^1$H NMR (400 MHz, $CDCl_3$) $\delta$ 7.36 – 7.24 (m, 18H, CH Ar), 7.22 – 7.19 (m, 2H, CH Ar), 4.94 (d, $J$ = 11.2 Hz, 1H, CH*H*Ph), 4.91 – 4.86 (m, 3H, CH*H*Ph), 4.79 (d, $J$ = 11.3 Hz, 1H, CH*H*Ph), 4.53 (d, $J$ = 10.8 Hz, 1H, CH*H*Ph), 4.45 (d, $J$ = 12.0 Hz, 1H, CH*H*Ph), 4.41 (d, $J$ = 12.0 Hz, 1H, CH*H*Ph), 3.76 (dd, $J$ = 9.3, 2.4 Hz, 1H, CH-7a), 3.68 – 3.62 (m, 2H, CH-6, CH-7b), 3.57 (t, $J$ = 9.2 Hz, 1H, CH-1), 3.38 (t, $J$ = 9.2 Hz, 1H, CH-2), 3.24 (t, $J$ = 9.5 Hz, 1H, CH-3), 2.79 (t, $J$ = 10.4 Hz, 1H, CH-4), 2.13 (s, 3H, OH, $NH_2$), 1.41 (tt, $J$ = 10.9, 2.5 Hz, 1H, CH-5). $^{13}$C NMR (101 MHz, $CDCl_3$) $\delta$ 140.4, 140.3, 140.2, 139.9 ($4C_q$ Ar), 130.3, 130.1, 130.1, 129.7, 129.6, 129.5, 129.4, 129.4, 129.3 (20CH Ar), 87.8 (C-1), 85.5 (C-2), 80.3 (C-6), 78.3 (C-3), 77.3, 77.2, 77.1, 74.7 ($4CH_2$Ph), 66.6 (C-7), 52.6 (C-4), 48.40 (C-5). HRMS: calcd. for $[C_{35}H_{40}NO_5]^+$ 554.29010; found 554.28976.

***Tert*-butyl ((1*S*,2*R*,3*R*,4*S*,5*S*,6*R*)-3,4,5-tris(benzyloxy)-2-((benzyloxy)methyl)-6 hydroxycyclohexyl) carbamate (21):** Amino alcohol **20** (74 mg, 0.13 mmol) was dissolved in anhydrous DCM (2.6 mL) and $Et_3N$ (93

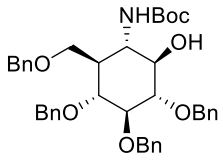


µL, 0.7 mmol, 5 eq) and $Boc_2O$ (37 µL, 0.16 mmol, 1.2 eq) were added at 0 ℃. The reaction was stirred overnight at rt. Then, the reaction was quenched with sat. aq. $NH_4Cl$ and the aqueous phase was extracted with DCM (3x). The combined organic layers were dried over $MgSO_4$, filtered and concentrated *in vacuo*. The crude product was purified by silica gel column chromatography (Pentane/EtOAc 100:1 → 6:4) to obtain **21** (66 mg, 0.1 mmol, 78%) as a colourless oil. $^1$H NMR (500 MHz, DMSO-$d_6$) δ 7.36 – 7.22 (m, 20H, CH Ar), 5.33 (dd, $J$ = 11.9, 4.9 Hz, 1H, CH*H*Ph), 4.67 (d, $J$ = 11.9 Hz, 1H, CH*H*Ph), 4.62 (d, $J$ = 12.1 Hz, 1H, CH*H*Ph), 4.56 (td, $J$ = 12.6, 11.9, 2.6 Hz, 4H, CH*H*Ph), 4.44 (d, $J$ = 1.1 Hz, 2H, CH*H*Ph), 4.41 – 4.38 (m, 1H, OH), 3.99 (dd, $J$ = 10.6, 2.9 Hz, 1H, CH-4), 3.95 (dd, $J$ = 5.5, 2.9 Hz, 1H, CH-3), 3.92 (t, $J$ = 3.3 Hz, 1H, CH-7b), 3.82 (dd, $J$ = 11.9, 2.6 Hz, 1H, CH-6), 3.78 (dd, $J$ = 10.7, 6.6 Hz, 1H, CH-7a), 3.15 (q, $J$ = 3.7, 2.5 Hz, 1H, CH-5), 1.46 (s, 9H, $(CH_3)_3$). $^{13}$C NMR (126 MHz, DMSO) δ 128.8, 128.7, 128.7, 128.5, 128.1, 128.00, 127.9, 127.9, 127.9, 127.8, 127.7 (CH Ar), 83.78 (C-3), 81.79 ($C(CH_3)_3$), 77.0, 75.6, 73.5, 73.0, 72.9, 72.6 ($4CH_2$Ph), 71.2 (C-6), 65.4 (C-7), 57.7 (C-1), 41.8 (C-5), 28.4 ($(CH_3)_3$). HRMS: calcd. for $[C_{40}H_{47}NO_7Na]^+$ 676.32447; found 654.32409.

**(1*R*,2*R*,3*S*,4*R*,5*R*,6*S*)-2,3,4-Tris(benzyloxy)-5-((benzyloxy)methyl)-6-((*tert*-butoxycarbonyl)amino) cyclohexyl ethanesulfonate (22):** Intermediate **21** (40 mg, 61 µmol) was dissolved in anhydrous DCM (0.6 mL)

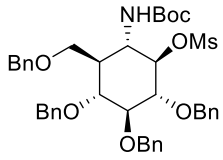


and $Et_3N$ (42 µL, 0.3 mmol, 5 eq), Me-imidazole (50 µL, 0.61 mmol, 10 eq) and MsCl (23 µL, 0.30 mmol, 5 eq) were added to the reaction at 0 ℃. The reaction was stirred at rt overnight. The reaction was diluted with EtOAc and washed with 1M HCl (3x), $H_2O$ and brine. The organic layer was dried over $MgSO_4$, filtered and concentrated *in vacuo*. The crude product was purified by silica gel column chromatography (Pentane/EtOAc 100:1 → 7:3) to obtain **22** (35,5 mg, 49 µmol, 80%) as a yellow oil and **32** as a white solid side product (4,5 mg, 8 µmol, 13%). $^1$H NMR (400 MHz, $CDCl_3$) $\delta$ 7.41 – 7.25 (m, 18H, CH Ar), 7.24 – 7.20 (m, 2H, CH Ar), 4.97 (d, $J$ = 10.9 Hz, 1H, CH*H*Ph), 4.94 – 4.87 (m, 3H, CH*H*Ph), 4.81 (d, $J$ = 10.9 Hz, 1H, CH*H*Ph), 4.68 (d, $J$ = 9.4 Hz, 1H, CH*H*Ph), 4.61 (d, $J$ = 10.7 Hz, 2H, CH*H*Ph, CH-1), 4.51 (d, $J$ = 11.5 Hz, 1H, CH*H*Ph), 4.41 (d, $J$ = 11.5 Hz, 1H, CH*H*Ph), 3.93 (dd, 1H, CH-6), 3.81 (dd, $J$ = 9.3, 2.6 Hz, 1H, CH-7a), 3.76 (ddd, $J$ = 10.3, 6.5, 2.7 Hz, 1H, CH-4), 3.67 – 3.60 (m, 2H, CH-3, CH-7b), 3.55 (dd, $J$ = 9.4, 2.1 Hz, 1H, CH-2), 2.89 (s, 3H, $CH_3$), 1.88 – 1.76 (m, 1H, CH-5), 1.48 (s, 9H, $(CH_3)_3$). $^{13}$C NMR (101 MHz, $CDCl_3$) $\delta$ 155.2 (C=O), 138.3, 138.2, 138.1, 137.8 ($4C_q$ Ar), 128.5, 128.5, 128.4, 128.0, 127.9, 127.8, 127.7, 127.7, 127.7 (20CH Ar), 85.6 (C-2/C-3), 83.8 (C-1), 80.8 (C-2/C-3), 77.8 (C-4), 75.7, 75.6, 75.5, 73.5 ($4CH_2$Ph), 64.9 (C-7), 50.0 (C-6), 44.2 (C-5), 38.8 ($CH_3$), 28.4 ($(CH_3)_3$). HRMS: calcd. for $[C_{41}H_{49}NNaO_9S]^+$ 754.30202; found 754.30184, calcd. for $[C_{41}H_{53}N_2O_9S]^+$ 749.34663; found 749.34652.

**(3a*S*,4*R*,5*R*,6*S*,7*S*,7a*R*)-5,6,7-Tris(benzyloxy)-4-((benzyloxy)methyl)hexahydrobenzo [*d*]oxazol-2(3*H*)-one (32):** $^1$H NMR (400 MHz, $CDCl_3$) δ 7.39 – 7.22 (m, 18H, $CH_{Ar}$), 7.20 – 7.15 (m, 2H, $CH_{Ar}$), 5.20 (s, 1H, NH), 4.95 (dd, *J* = 11.1, 5.3 Hz, 2H, 2x CH*H*Ph), 4.81 (d, *J* = 11.0 Hz, 1H, CH*H*Ph), 4.74 (d, *J* = 10.8 Hz, 1H, CH*H*Ph), 4.70 (d, *J* = 11.4 Hz, 1H, CH*H*Ph), 4.45 (d, *J* = 11.0 Hz, 1H, CH*H*Ph), 4.40 (s, 2H, 2x CH*H*Ph), 4.10 (dd, *J* = 11.7, 9.8 Hz, 1H, C-3), 3.86 (dd, *J* = 9.9, 7.6 Hz, 1H, CH-1), 3.72 (t, *J* = 8.0 Hz, 1H, CH-2), 3.58 (dd, *J* = 9.5, 3.8 Hz, 2H, CH-7), 3.49 (dd, *J* = 9.5, 8.4 Hz, 1H, CH-4), 3.44 (dd, *J* = 9.5, 6.6 Hz, 1H, CH-7), 3.40 – 3.33 (m, 1H, CH-6), 2.01 (tdd, *J* = 13.2, 6.6, 3.8 Hz, 1H, CH-5). $^{13}$C NMR (101 MHz, $CDCl_3$) δ 160.0 ($C_{q\ carbamate}$), 138.2, 137.9, 137.9, 137.5 ($4C_q$), 128.8, 128.6, 128.58, 128.5, 128.3, 128.2, 128.1, 128.08, 128.0, 127.97, 127.9 (11*C*$H_{Ar}$), 85.9 (C-2), 83.6 (C-3), 80.1 (C-1), 79.6 (C-4), 76.0, 75.4, 73.5 ($4CH_2Ph$), 68.7 (C-7), 56.1 (C-6), 43.5 (C-5). HRMS: calcd. For $[C_{36}H_{41}N_2O_6]^+$ 597.29591; found 597.29572, calcd. For $[C_{36}H_{37}NnaO_6]^+$ 602.25131; found 602.25126.

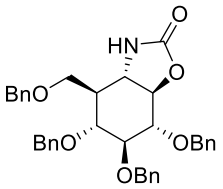


**3a*S*,4*R*,5*R*,6*S*,7*S*,7a*S*)-5,6,7-Tris(benzyloxy)-4-((benzyloxy)methyl)hexahydrobenzo-[*d*]oxazol-2(3*H*)-one (23):** Intermediate **22** (89 mg, 0.12 mmol) was dissolved in anhydrous DMF (5.6 mL). The reaction mixture was stirred for 24 h at 120 ℃. The reaction was cooled to rt and diluted with $H_2O$. The aqueous phase was extracted with EtOAc (3x) and the combined organic layers were washed with $H_2O$ (2x) and brine, dried over $MgSO_4$, filtered and concentrated *in vacuo*. The crude product was purified by silica gel column chromatography (Pent/EtOAc 100:1 → 50:50) to obtain **23** (60 mg, 0.11 mmol, 85%) as a white solid. $^1$H NMR (400 MHz, $CDCl_3$) *δ* 7.41 – 7.24 (m, 16H, CH Ar), 7.24 – 7.20 (m, 2H CH Ar), 7.20 – 7.14 (m, 2H, CH Ar), 5.67 (s, 1H, NH), 4.79 (d, *J* = 12.0 Hz, 1H, CH*H*Ph), 4.71 (dd, *J* = 8.7, 3.7 Hz, 1H, CH-1), 4.64 (d, *J* = 12.1 Hz, 1H, CH*H*Ph), 4.60 (d, *J* = 11.5 Hz, 1H, CH*H*Ph), 4.48 (dd, *J* = 11.6, 4.4 Hz, 2H, CH*H*Ph), 4.43 – 4.34 (m, 3H, CH*H*Ph), 3.87 (t, *J* = 3.7 Hz, 1H, CH-2), 3.82 – 3.75 (m, 3H, CH-3, CH-6, CH-7a), 3.29 (t, *J* = 9.0 Hz, 1H, CH-4), 3.24 (dd, *J* = 12.0, 5.5 Hz, 1H, CH-7b), 2.61 (dtd, *J* = 12.8, 9.1, 3.8 Hz, 1H, CH-5). $^{13}$C NMR (101 MHz, $CDCl_3$) *δ* 158.7 (C=O), 138.0, 137.8, 137.7, 137.6 ($4C_q$ Ar), 128.7, 128.7, 128.6, 128.5, 128.3, 128.2, 128.1, 128.1, 128.0, 127.9 (20CH Ar), 81.9 (C-3/C-6), 78.3 (C-4), 75.7 (C-2), 74.8 (C-1), 73.7, 73.0, 72.6 ($3CH_2Ph$), 71.5 (C-7), 54.4 (C-3/C-6), 42.5 (C-5). HRMS: calcd. For $[C_{36}H_{41}N_2O_6]^+$ 597.29591; found 597.29572, calcd. For $[C_{36}H_{37}NnaO_6]^+$ 602.25131; found 602.25110.

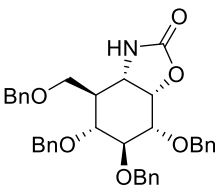


**(1*S*,2*S*,3*R*,4*R*,5*S*,6*S*)-2-Amino-4,5,6-tris(benzyloxy)-3-((benzyloxy)methyl)cyclohexan-1-ol (24):** Cyclic carbamate **23** (60 mg, 0.11 mmol) was dissolved in EtOH (6.6 mL) and NaOH (1M, 1.65 mL, 1.65 mmol, 15 eq) was added to the solution. The reaction mixture was stirred at 70 ℃ for 3 h and was subsequently stirred overnight at rt. After 24 h extra NaOH (1M, 1.65 mL, 1.65 mmol, 15 eq) was added and the reaction was again heated to 70 ℃ and stirred for 3 h followed by overnight stirring at rt.. The reaction mixture was concentrated and the crude residue was diluted with $H_2O$. The aqueous phase was extracted with EtOAc (3x) and the combined organic layers were washed with $H_2O$ and brine, dried over $MgSO_4$, filtered and concentrated *in vacuo*. The crude product was purified by silica gel column chromatography (DCM/MeOH 100:1 → 85:15) to obtain **24** (50 mg, 90 µmol, 82%) as a colourless oil. $^1$H NMR (500 MHz, $CDCl_3$) *δ* 7.37 – 7.24 (m, 18H, CH Ar), 7.22 – 7.18 (m, 2H, CH Ar), 4.91 (d, *J* = 10.8 Hz, 1H, CH*H*Ph), 4.88 (d, *J* = 10.9 Hz, 1H, CH*H*Ph), 4.81 (d, *J* = 10.8 Hz, 1H, CH*H*Ph), 4.71 (d, 1H, CH*H*Ph), 4.70 (d, 1H, CH*H*Ph), 4.48 (d, *J* = 10.9 Hz, 1H, CH*H*Ph), 4.43 (s, 2H, CH*H*Ph), 4.12 (t, *J* = 2.7 Hz, 1H, CH-1), 3.90 (t, *J* = 9.4 Hz, 1H, CH-3), 3.75 (dd, *J* = 9.5, 3.2 Hz, 1H, CH-7a), 3.67 (dd, *J* = 9.5, 2.6 Hz, 1H, CH-7b), 3.49 (dd, *J* = 10.8, 9.3 Hz, 1H, CH-4), 3.43 (dd, *J* = 9.5, 2.7 Hz, 1H, CH-2), 2.92 (dd, *J* = 10.9, 2.5 Hz, 1H, CH-6), 2.64 (s, 3H, $NH_2$, OH), 1.97 (tt, *J* = 11.0, 2.9 Hz, 1H, CH-5). $^{13}$C NMR (126 MHz, $CDCl_3$) *δ* 139.0, 138.7, 138.3, 138.1 ($4C_q$ Ar), 128.6, 128.6, 128.5, 128.5, 128.1, 128.1, 128.0, 127.9, 127.7, 127.6 (20CH Ar), 83.3 (C-3), 81.3 (C-2), 78.7 (C-4), 75.8, 75.5, 73.2, 72.6 ($4CH_2Ph$), 70.9 (C-1), 66.3 (C-7), 49.9 (C-6), 43.4 (C-5). HRMS: calcd. for $[C_{35}H_{40}NO_5]^+$ 554.29010; found 554.28970.

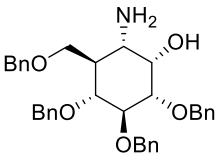

***Tert*-butyl (3a*S*,4*R*,5*R*,6*S*,7*R*,7a*S*)-5,6,7-tris(benzyloxy)-4-((benzyloxy)methyl) hexahydro-3*H*-benzo[*d*][1,2,3]oxathiazole-3-carboxylate 2,2-dioxide (25):** The amino alcohol **24** (50 mg, 90 µmol) was dissolved in anhydrous DCM (1.67 mL). $Et_3N$ (63 µL, 0.45 mmol, 5 eq) and $Boc_2O$ (25 µL, 0.11 mmol, 1.2 eq) were added at 0 °C and the reaction was stirred overnight at rt. The reaction was then quenched with sat. aq. $NH_4Cl$ and the aqueous phase was extracted with DCM (3x). The combined organic layers were dried over $MgSO_4$, filtered and concentrated *in vacuo*. The Boc proctected intermediate was dissolved in anhydrous DCM (1.67 mL) and $Et_3N$ (132 µL, 0.95 mmol, 10.5 eq), imidazole (34 mg, 0.50 mmol, 5.5 eq) and $SOCl_2$ (66µL, 0.9 mmol, 10 eq) were added at 0 °C and the reaction was stirred at rt for 20 min. $H_2O$ was added to the reaction mixture and the aqueous phase was extracted with DCM (3x). The combined organic layers were dried over $MgSO_4$, filtered and concentrated *in vacuo*. The crude mixture of sulfites was dissolved in a 1:1:1 mixture of $H_2O$ (1.3 mL), EtOAc (1.3 mL) and MeCN (1.3 mL), and $NaIO_4$ (48 mg, 0.23 mmol, 2.5 eq) and $RuCl_3 \cdot H_2O$ (4.7 mg, 23 µmol, 0.25 eq) were added at 0 °C and the reaction was stirred at this temperature for 1h. The reaction was quenched with sat. aq. $Na_2S_2O_3$ and the aqueous phase was extracted with EtOAc (3x). The combined organic layers were washed with brine, dried over $MgSO_4$, filtered and concentrated *in vacuo*. The crude product was purified by silica gel column chromatography (Pentane/EtOAc 100:1 → 90:10) to obtain **25** (21 mg, 30 µmol, 33% over 3 steps) as a colourless oil. $^1$H NMR (400 MHz, $CDCl_3$) $\delta$ 7.37 – 7.23 (m, 18H, CH Ar), 7.19 – 7.14 (m, 2H, CH Ar), 4.99 (t, $J$ = 3.6 Hz, 1H, CH-1), 4.92 (d, $J$ = 10.7 Hz, 1H, CH*H*Ph), 4.91 – 4.84 (m, 2H, CH*H*Ph), 4.79 (d, $J$ = 11.9 Hz, 1H, CH*H*Ph), 4.74 (d, $J$ = 11.9 Hz, 1H, CH*H*Ph), 4.66 (dd, $J$ = 10.4, 3.9 Hz, 1H, CH-6), δ 4.52 (d, $J$ = 11.3 Hz, 1H, CH*H*Ph), 4.35 (d, $J$ = 11.3 Hz, 1H, CH*H*Ph), 3.94 (t, 1H, CH-3), 3.91 – 3.88 (m, 1H, CH-7a), 3.63 (dd, $J$ = 7.0, 2.9 Hz, 1H, CH-4), 3.59 (dd, $J$ = 1.8 Hz 1H, CH-2), 3.34 (dd, $J$ = 9.5, 1.9 Hz, 1H, CH-7b), 2.22 (tt, 1H, CH-5), 1.55 (s, 9H $(CH_3)_3$). $^{13}$C NMR (101 MHz, $CDCl_3$) $\delta$ 149.0 (C=O), 138.5, 138.4, 138.2, 137.2 ($4C_q$ Ar), 128.8, 128.6, 128.5, 128.5, 128.4, 128.2, 128.2, 128.0, 127.9, 127.8 (20CH Ar), 85.7 ($CH_2$Ph), 81.9 (C-3), 80.7 (C-1), 76.8 (C-2/C-4) 76.5 (C-2/C-4), 76.1, 75.8, 73.6 ($3CH_2$Ph), 64.7 (C-7), 56.1 (C-6), 45.4 (C-5), 28.0 ($(CH_3)_3$). HRMS: calcd. for $[C_{40}H_{45}NO_9SNa]^+$ 738.27072; found 738.27000, calcd. for $[C_{40}H_{49}N_2O_9S]^+$ 733.31533; found 733.31472.

**(3a*S*,4*R*,5*R*,6*S*,7*R*,7a*S*)-5,6,7-Tris(benzyloxy)-4-((benzyloxy)methyl)hexahydro-3*H* benzo[*d*][1,2,3]oxathiazole 2,2-dioxide (26):** Cyclosulfamidate **25** (20 mg, 30 µmol) was dissolved in anhydrous DCM (1.2 mL) and TFA (0.11 mL) was added to the reaction mixture. The reaction was stirred overnight at rt. Then, the reaction mixture was diluted with $H_2O$ and the aqueous phase was extracted with DCM (3x). The combined organic layers were dried over $MgSO_4$, filtered and concentrated *in vacuo*. The crude product was purified by silica gel column chromatography (Pent/EtOAc 95:5 → 70:30) to obtain **26** (13 mg, 21 µmol, 65%) as a colourless oil. $^1$H NMR (400 MHz, $CDCl_3$) $\delta$ 7.40 – 7.22 (m, 18H, CH Ar), 7.21 – 7.14 (m, 2H, CH Ar), 4.85 (dd, $J$ = 5.6, 3.1 Hz, 1H, CH-1), 4.77 (d, $J$ = 11.0 Hz, 1H, CH*H*Ph), 4.73 (d, $J$ = 11.7 Hz, 1H, CH*H*Ph), 4.71 – 4.60 (m, 3H, CH*H*Ph), 4.59 (d, $J$ = 11.1 Hz, 1H, CH*H*Ph), 4.48 (dd, $J$ = 20.9, 9.7 Hz, 3H, CH*H*Ph), 4.07 (ddd, $J$ = 10.0, 8.2, 5.5 Hz, 1H, CH-6), 3.88 (dd, $J$ = 7.6, 5.5 Hz, 1H, CH-3), 3.77 (dd, $J$ = 5.6, 3.0 Hz, 1H, CH-2), 3.73 (dd, $J$ = 9.3, 3.9 Hz, 1H, CH-7a), 3.61 (dd, $J$ = 9.2, 2.5 Hz, 1H, CH-7b), 3.52 (dd, $J$ = 11.8, 7.6 Hz, 1H, CH-4), 2.33 (tt, $J$ = 12.2, 3.2 Hz, 1H, CH-5), 1.56 (s, 1H, NH). $^{13}$C NMR (101 MHz, $CDCl_3$) $\delta$ 138.2, 137.8, 137.7, 137.1, ($4C_q$ Ar) 128.8, 128.7, 128.7, 128.6, 128.5, 128.5, 128.1, 128.1, 128.1, 128.0, 128.0, 127.9 (20CH Ar), 82.4 (C-1), 82.1 (C-3), 77.2 (C-2), 76.9 (C-4), 74.9, 74.1, 73.7, 73.5 ($4CH_2$Ph), 66.6 (C-7), 55.8 (C-6), 42.8 (C-5). HRMS: calcd. for $[C_{35}H_{37}NO_7SNa]^+$ 638.21829; found 638.21792, calcd. for $[C_{35}H_{41}N_2O_7S]^+$ 633.26290; found 633.26263.

**(3a*S*,4*R*,5*R*,6*S*,7*R*,7a*S*)-5,6,7-Tris(benzyloxy)-4-((benzyloxy)methyl)-3-methyl hexahydro-*3H*-benzo[*d*][1,2,3]oxathiazole 2,2-dioxide (27):** $K_2CO_3$ (5.64 mg, 41 µmol 1.2 eq), TBAI (1.26 mg 0.1 eq) and iodomethane (4.25 µL, 68 µmol, 2 eq) were added to a solution of **26** (21 mg, 34 µmol) in anhydrous DMF (1 mL) and the reaction was stirred at rt for 5 h. The reaction mixture was diluted with EtOAc and $H_2O$ and the aqueous phase was extracted with EtOAc (3x). The combined organic layers were washed with water and brine, dried over $MgSO_4$, filtered and concentrated *in vacuo*. The crude product was purified by silica gel column chromatography (Pent/EtOAc 100:1 → 85:15) to afford **27** (17 mg, 27 µmol, 79%) as a

colourless oil. $^1$H NMR (500 MHz, $CDCl_3$) $\delta$ 7.38 – 7.24 (m, 18H, $CH_{Ar}$), 7.24 – 7.21 (m, 2H, $CH_{Ar}$), 4.92 – 4.85 (m, 3H, 2x CH*H*Ph, C-1), 4.81 (d, *J* = 10.8 Hz, 1H, CH*H*Ph), 4.76 (s, 2H, 2x CH*H*Ph), 4.52 (d, *J* = 11.0 Hz, 1H, CH*H*Ph), 4.44 (d, *J* = 11.7 Hz, 1H, CH*H*Ph), 4.31 (d, *J* = 11.8 Hz, 1H, CH*H*Ph), 3.91 (t, *J* = 9.3 Hz, 1H, C-3), 3.83 (dd, *J* = 9.4, 2.2 Hz, 1H, C-7), 3.59 (dd, *J* = 9.5, 3.7 Hz, 1H, C-2), 3.58 – 3.51 (m, 2H, C-6, C-7), 3.48 (dd, *J* = 11.4, 9.1 Hz, 1H, C-4), 2.70 (s, 3H, $CH_3$), 2.28 (tt, *J* = 11.1, 2.2 Hz, 1H, C-5). $^{13}$C NMR (126 MHz, $CDCl_3$) $\delta$ 138.5, 138.4, 137.8, 137.5 ($4C_q$), 128.7, 128.7, 128.56, 128.3, 128.2, 128.2, 128.15, 128.1, 127.89, 127.85, 127.8 (11 $CH_{Ar}$), 82.1 (C-3), 76.9 (C-2), 76.6 (C-4), 75.9, 75.4, 73.4, 73.3 ($4CH_2Ph$), 64.5 (C-7), 62.1 (C-6), 44.7 (C-5), 36.8 (*C*$H_3$). ). HRMS: calcd. for $[C_{36}H_{39}NO_7SNa]^+$ 652.23394; found 652.23376.

**(3a*S*,4*R*,5*R*,6*S*,7*R*,7a*S*)-5,6,7-Trihydroxy-4-(hydroxymethyl)hexahydro-3*H*-benzo[*d*]-[1,2,3]oxathiazole 2,2-dioxide (6):** Perbenzylated **26** (13 mg, 21 µmol) was dissolved in MeOH (1 mL) and the solution was purged with $N_2$. Pd/C (10 wt %, 16 mg, 15 µmol, 0.7 eq) was added , the solution was purged with $N_2$ and the reaction was stirred overnight under $H_2$ atmosphere at rt. The reaction was flushed with $N_2$, filtered over a celite plug and concentrated *in vacuo*. The crude product was purified by silica gel column chromatography (DCM/MeOH 100:1 → 80:20) to obtain **6** (4.66 mg, 18.27 µmol, 87%) as a white solid. $^1$H NMR (500 MHz, MeOD) $\delta$ 4.95 (t, 1H, CH-1), 3.98 (dd, *J* = 11.0, 2.6 Hz, 1H, CH-7a), 3.87 (dd, *J* = 11.1, 4.0 Hz, 1H, CH-6), 3.67 (dd, *J* = 11.0, 2.9 Hz, 1H, CH-7b), 3.61 – 3.55 (m, 2H, CH-2, CH-3), 3.39 – 3.35 (m, 1H, CH-4), 1.96 (tt, *J* = 11.2, 8.4, 2.7 Hz, 1H, CH-5). $^{13}$C NMR (126 MHz, MeOD) $\delta$ 88.5 (C-1), 74.9 (C-2/C-3), 71.7 (C-2/C-3), 70.3 (C-4), 58.3 (C-7), 56.5 (C-6), 46.2 (C-5). HRMS: calcd. for $[C_7H_{14}N_1O_7S]^+$ 256,04855; found 256,04820.

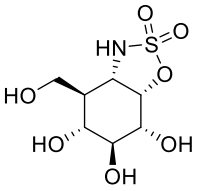

**(3a*S*,4*R*,5*R*,6*S*,7*R*,7a*S*)-5,6,7-trihydroxy-4-(hydroxymethyl)-3-methylhexahydro-3*H*-benzo[*d*][1,2,3]oxathiazole 2,2-dioxide (7):** Perbenzylated **27** (17 mg, 27 µmol) was dissolved in a MeOH (1.2 mL), purged with $N_2$ and Pd/C (10 wt %, 17 mg, 16 µmol, 0.6 eq) was added and the reaction mixture was purged again with $N_2$. The reaction was stirred overnight under $H_2$ atmosphere at rt. The reaction mixture was flushed with $N_2$, filtered over a celite plug and concentrated *in vacuo*. The crude product was purified by silica gel column chromatography (DCM/MeOH 100:1 → 80:20) to obtain **7** (6.1 mg, 24 µmol, 89%) as a white solid. $^1$H NMR (500 MHz, MeOD) $\delta$ 5.05 – 5.03 (m, 1H, CH-1), 4.04 (dd, *J* = 11.1, 2.3 Hz, 1H, CH-7B), 3.72 (dd, *J* = 10.9, 4.0 Hz, 1H, CH6), 3.67 (dd, *J* = 11.1, 2.8 Hz, 1H, CH-7A), 3.61 – 3.52 (m, 2H, CH-2, CH-3), 3.37 – 3.33 (m, 1H, CH-4), 2.94 (s, 3H, $CH_3$), 1.96 (tt, *J* = 11.1, 2.6 Hz, 1H, CH-5). $^{13}$C NMR (126 MHz, MeOD) $\delta$ 83.3 (C-1), 73.6 (C2/3), 70.0 (C2/3), 68.6 (C-4), 62.3 (C-6), 56.4 (C-7), 46.2 (C-5), 36.1 (*C*$H_3$). HRMS: calcd. for $[C_8H_{16}NO_7S]^+$ 270.06420; found 270.06377.

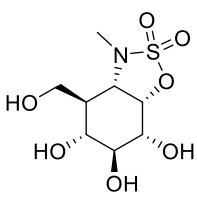

**Synthesis and characterization data of 8**

**(1*R*,2*R*,3*S*,4*S*,5*R*,6*R*)-2-Azido-3,4,5-tris(benzyloxy)-6-((benzyloxy)methyl)cyclohexyl methanesulfonate (32):** Azide **10** (50 mg, 86 µmol) was dissolved in anhydrous DCM (1 mL) and $Et_3N$ (60 µL, 0.43 mmol, 5 eq), Me-Imidazole (69 µL, 0.86 mmol, 10 eq) and MsCl (33 µL, 0.43 mmol, 5 eq) were added to the solution at 0 °C. The reaction was stirred for 3 h at rt. The reaction mixture was diluted with EtOAc and the organic phase was washed with 1M HCl (3x), $H_2O$ and brine, dried over $MgSO_4$, filtered and concentrated *in vacuo*. The crude product was purified by silica gel column chromatography (Pentane/EtOAc 100:1→75:25) to obtain **32** (49 mg, 75 µmol, 87%) as a colourless oil. $^1$H NMR (500 MHz, $CDCl_3$) $\delta$ 7.38 – 7.25 (m, 18H, CH Ar), 7.19 – 7.16 (m, 2H, CH Ar), 4.95 (d, *J* = 10.7 Hz, 1H), 4.88 – 4.84 (m, 2H, CH*H*Ph, CH-6), 4.80 (d, *J* = 10.7 Hz, 1H, CH*H*Ph), 4.76 (d, *J* = 11.5 Hz, 1H, CH*H*Ph), 4.72 (d, *J* = 11.5 Hz, 1H, CH*H*Ph), 4.47 – 4.42 (m, 2H, CH*H*Ph), 4.40 (d, *J* = 11.8 Hz, 1H, CH*H*Ph), 4.23 (t, *J* = 3.7 Hz, 1H, CH-1), 3.98 (dd, *J* = 9.6, 3.4 Hz, 1H, CH-2), 3.90 (t, *J* = 9.3 Hz, 1H, CH-3), 3.72 (dd, *J* = 9.5, 4.3 Hz, 1H, CH-7B), 3.42 (dd, *J* = 11.4, 8.8 Hz, 1H, CH-4), 3.34 (t, *J* = 9.9 Hz, 1H, CH-7A), 2.83 (s, 3H, C*H*$_3$), 2.39 (dddd, *J* = 11.3, 10.3, 4.3, 2.6 Hz, 1H, CH-5). $^{13}$C NMR (126 MHz, $CDCl_3$) $\delta$ 138.6, 138.01, 137.6, 137.6 ($4C_q$ Ar), 128.7, 128.6, 128.6, 128.5, 128.3, 128.2, 128.1, 128.0, 128.0, 128.0, 128.0, 127.8 (20CH Ar), 83.2 (C-3), 79.2 (C-2), 77.7 (C-4), 77.1 (C-6), 76.0, 75.5, 73.6, 73.3 ($4CH_2Ph$), 66.3 (C-7), 60.9 (C-1), 40.4 (C-5), 37.6 (*C*$H_3$). HRMS: calcd. for $[C_{36}H_{39}N_3O_7SNa]^+$ 680.24009; found 680.23969, calcd. for $[C_{36}H_{43}N_4O_7S]^+$ 675.28470; found 675.28427.

**(1*R*,2*S*,3*R*,4*R*,5*S*,6*R*)-2-azido-4,5,6-tris(benzyloxy)-3-((benzyloxy)methyl)cyclohexyl methanesulfonate (28):** Azide **19** (0.11 g, 0.19 mmol) was dissolved in anhydrous DCM (1.73 mL) and $Et_3N$ (0.13 mL, 0.95 mmol, 5 eq), methyl imidazole (0.15 mL, 1.9 mmol, 10 eq) and MsCl (74 µL, 0.95 mmol, 5 eq) were added to the solution at 0 °C. The reaction was stirred for 3 h at rt. The reaction mixture was diluted with EtOAc and the organic phase was washed with 1M HCl (3x), $H_2O$ and brine, dried over $MgSO_4$, filtered and concentrated *in vacuo*. The crude product was purified by silica gel column chromatography (Pentane/EtOAc 100:1→75:25) to obtain **28** (0.11 g, 0.17 mmol, 88%) as a white solid. $^1$H NMR (500 MHz, $CDCl_3$) $\delta$ 7.37 – 7.22 (m, 18H, CH Ar), 7.18 – 7.15 (m, 2H, CH Ar), 4.90 – 4.82 (m, 5H, CH*H*Ph), 4.52 – 4.46 (m, 3H, CH*H*Ph, CH-1), 4.40 (d, *J* = 11.5 Hz, 1H, CH*H*Ph), 3.84 (dd, *J* = 9.4, 1.8 Hz, 1H, CH-7B), 3.75 – 3.70 (m, 1H, CH-6), 3.70 – 3.65 (m, 2H, CH-3, CH-7A), 3.59 – 3.53 (m, 2H, CH-2, CH-4), 2.99 (s, 3H, C*H*$_3$), 1.59 (tt, *J* = 11.3, 2.2 Hz, 1H, CH-5). $^{13}$C NMR (126 MHz, $CDCl_3$) $\delta$ 138.1, 138.0, 137.7, 137.6 (4C$_q$ Ar), 128.6, 128.6, 128.6, 128.5, 128.1, 128.1, 128.0, 128.0, 127.9, 127.8, 127.7 (CH Ar), 85.5 (C-2/C-4), 83.8 (C-1), 80.5 (C-2/C-4), 77.1 (C-3), 75.9, 75.8, 75.8, 73.4 (4$CH_2$Ph), 64.6 (C-7), 60.5 (C-6), 44.6 (C-5), 39.2 (*C*H$_3$). HRMS: calcd. for $[C_{36}H_{39}N_3O_7SNa]^+$ 680.24009; found 680.23974, calcd. for $[C_{36}H_{43}N_4O_7S]^+$ 675.28470; found 675.28437.

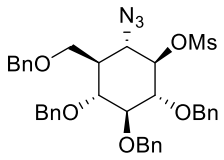


**((((1*R*,2*S*,3*S*,4*S*,5*S*,6*R*)-4,5-Diazido-6-((benzyloxy)methyl)cyclohexane-1,2,3-triyl)tris-(oxy))tris(methylene))tribenzene (29):** Mesylate **28** (0.1 g, 0.15 mmol) was dissolved in anhydrous DMF (4 mL) and $NaN_3$ (0.1 g, 1.5 mmol, 10 eq) was added and the reaction was stirred for 18 h at 100 °C. The reaction mixture was cooled to rt and EtOAc and $H_2O$ were added to the reaction mixture. The aqueous layers was extracted with EtOAc (2x). The combined organic layers were washed with $H_2O$ and brine, dried over $MgSO_4$, filtered and concentrated *in vacuo*. The crude product was purified by silica gel column chromatography (Pentane/EtOAc 100:1→70:30) to obtain **29**[50] (67 mg, 0.11 mmol, 71%) as a white solid. $^1$H NMR (500 MHz, $CDCl_3$) $\delta$ 7.38 – 7.24 (m, 18H, CH Ar), 7.20 – 7.16 (m, 2H, CH Ar), 4.93 (d, *J* = 10.6 Hz, 1H, CH*H*Ph)), 4.88 (d, *J* = 10.8 Hz, 1H, CH*H*Ph), 4.80 (d, *J* = 10.7 Hz, 1H, CH*H*Ph), 4.75 (d, *J* = 11.7 Hz, 1H, CH*H*Ph), 4.71 (d, *J* = 11.7 Hz, 1H, CH*H*Ph), 4.48 (d, *J* = 7.4 Hz, 1H, CH*H*Ph), 4.45 (d, *J* = 6.6 Hz, 1H, CH*H*Ph), 4.34 (d, *J* = 11.5 Hz, 1H, CH*H*Ph), 4.06 (t, *J* = 3.1 Hz, 1H, CH-1), 3.87 (t, *J* = 9.4 Hz, 1H, CH-3), 3.83 (dd, *J* = 9.5, 1.8 Hz, 1H, CH-7B), 3.56 (ddd, *J* = 9.2, 6.6, 4.0 Hz, 2H, CH-4, CH-7A), 3.53 – 3.49 (m, 2H, CH-2, CH-6), 2.03 (tt, *J* = 11.1, 2.2 Hz, 1H, CH-5). $^{13}$C NMR (126 MHz, $CDCl_3$) $\delta$ 138.6, 138.4, 138.0, 137.6 (4C$_q$ Ar), 128.7, 128.5, 128.5, 128.2, 128.1, 128.1, 128.0, 128.0, 127.8, 127.8 (20CH Ar), 83.1 (C-3), 80.3 (C-2), 77.6 (C-4), 76.0, 75.7, 73.3, 73.2 (4$CH_2$Ph), 65.0 (C-7), 63.6 (C-1), 57.6 (C-6), 42.5 (C-5). HRMS: calcd. For $[C_{36}H_{35}N_6O_4Na]^+$ 627.26902; found 627.26879, calcd. For $[C_{36}H_{39}N_7O_4]^+$ 622.31363; found 622.31346.

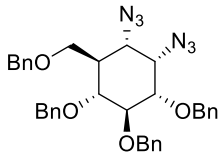


**(1*S*,2*S*,3*S*,4*S*,5*R*,6*R*)-3,4,5-Tris(benzyloxy)-6-((benzyloxy)methyl)cyclohexane-1,2-diamine (30):** Diazo-compound **29** (80 mg, 0.13 mmol) was dissolved in anhydrous THF (4.6 mL) and the solution was purged with $N_2$. $PtO_2$ (12 mg, 52 µmol, 0.4 eq) was added and again the reaction mixture was purged with $N_2$. The reaction mixture was stirred under $H_2$ atmosphere for 3 h at rt. The reaction was flushed with $N_2$, filtered over a celite plug and concentrated *in vacuo* to obtain **30** (66 mg, 0.12 mmol, 92%) as a colourless oil. $^1$H NMR (500 MHz, $CDCl_3$) $\delta$ 7.37 – 7.21 (m, 20H, CH Ar), 4.93 (d, *J* = 10.7 Hz, 1H, CH*H*Ph), 4.90 (d, *J* = 10.9 Hz, 1H, CH*H*Ph), 4.80 (d, *J* = 10.7 Hz, 1H, CH*H*Ph), 4.69 (d, *J* = 11.7 Hz, 1H, CH*H*Ph), 4.65 (d, *J* = 11.7 Hz, 1H, CH*H*Ph), 4.50 (d, *J* = 10.9 Hz, 1H, CH*H*Ph), 4.44 (d, *J* = 12.0 Hz, 1H, CH*H*Ph), 4.40 (d, *J* = 12.0 Hz, 1H, CH*H*Ph), 3.92 (t, *J* = 9.3 Hz, 1H, CH-3), 3.78 (dd, *J* = 9.5, 2.6 Hz, 1H, CH-7B), 3.62 (dd, *J* = 9.4, 2.6 Hz, 1H, CH-7A), 3.53 (dd, *J* = 10.9, 9.2 Hz, 1H, CH-4), 3.46 (dd, *J* = 9.5, 3.8 Hz, 1H, CH-2), 3.43 (t, *J* = 3.5 Hz, 1H, CH-1), 2.85 (dd, *J* = 11.0, 3.1 Hz, 1H, CH-6), 1.93 (tt, *J* = 11.0, 2.6 Hz, 1H, CH-5), 1.35 (s, 4H, 2$NH_2$). $^{13}$C NMR (126 MHz, $CDCl_3$) $\delta$ 139.2, 139.0, 138.6, 138.6 (4C$_q$ Ar), 128.5, 128.5, 128.4, 128.1, 128.0, 127.8, 127.8, 127.6, 127.6 (20CH Ar), 83.2 (C-4), 81.8 (C-2), 79.1 (C-3), 75.7, 75.3, 73.1, 72.1 (4$CH_2$Ph), 66.0 (C-7) , 53.7 (C-1), 49.4 (C-6), 43.8 (C-5). HRMS: calcd. for $[C_{35}H_{41}N_2O_4]^+$ 553.30608; found 553.30560.

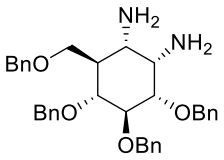

**(3a*S*,4*S*,5*S*,6*R*,7*R*,7a*S*)-4,5,6-Tris(benzyloxy)-7-((benzyloxy)methyl)octahydrobenzo[*c*] [1,2,5]thiadiazole 2,2-dioxide (31):** Diamine **30 (**51 mg, 92 µmol) was dissolved in anhydrous pyridine (10 mL) and sulfamide (18 mg, 1.85 mmol, 20 eq) was added to the reaction solution. The reaction was refluxed for 6 h. After completion the reaction mixture was concentrated *in vacuo* and coevaporated with toluene (3x). The crude product was dissolved in DCM, $H_2O$ was added and the aqueous layer was extracted with DCM (3x). The combined organic layers were dried over $MgSO_4$, filtered and concentrated *in vacuo*. The crude product was purified by silica gel column chromatography (Pentane/EtOAc 95:5→70:30) to obtain **31** (51 mg, 84 µmol, 91%) as a colourless oil. $^1$H NMR (500 MHz, $CDCl_3$) $\delta$ 7.36 – 7.24 (m, 18H, CH Ar), 7.21 – 7.17 (m, 2H, CH Ar), 4.85 (d, $J$ = 5.1 Hz, 1H, (NH), 4.77 (d, $J$ = 11.1 Hz, 1H, CH*H*Ph), 4.74 – 4.68 (m, 3H, CH*H*Ph), 4.64 – 4.59 (m, 2H, CH*H*Ph, NH), 4.48 – 4.42 (m, 2H, CH*H*Ph), 4.40 (d, $J$ = 11.9 Hz, 1H, CH*H*Ph), 4.14 (q, $J$ = 5.2 Hz, 1H, CH-1), 3.90 (t, $J$ = 7.3 Hz, 1H, CH-3), 3.76 (dt, $J$ = 10.7, 5.4 Hz, 1H, CH-6), 3.69 – 3.65 (m, 2H, CH-2, C-7B), 3.60 (dd, $J$ = 9.3, 5.0 Hz, 1H, CH-7A), 3.41 (dd, $J$ = 11.3, 7.5 Hz, 1H, CH-4), 2.40 (tdd, $J$ = 11.0, 5.0, 2.7 Hz, 1H, CH-5). $^{13}$C NMR (126 MHz, $CDCl_3$) $\delta$ 138.2, 138.1, 137.8, 137.3 ($4C_q$ Ar), 128.8, 128.7, 128.6, 128.6, 128.4, 128.2, 128.0, 128.0, 128.0, 127.9 (20CH Ar), 81.1 (C-3), 77.4 (C-4), 77.3 (C-2), 74.6, 74.6, 73.4, 73.3 ($4CH_2$Ph), 67.7 (C-7), 57.7 (C-1), 56.1 (C-6), 42.9 (C-5). HRMS: calcd. for $[C_{35}C_{39}N_2O_6S]^+$ 615.25233; found 615.25204.

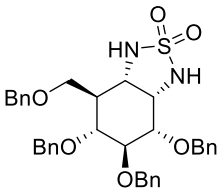


**(3a*S*,4*S*,5*S*,6*R*,7*R*,7a*S*)-4,5,6-Trihydroxy-7-(hydroxymethyl)octahydrobenzo[*c*][1,2,5] thiadiazole 2,2-dioxide (8):** Cyclosulfamide **31** (30 mg, 49 µmol) was dissolved in a 4:1 mixture of Methanol (2 mL) and DCM (0.5 mL), purged with $N_2$. Pd/C (10 wt%, 43 mg, 40 µmol, 0.8 eq) was added and the reaction mixture was purged again with $N_2$. The reaction was stirred for 18 h under $H_2$ atmosphere at rt. The reaction mixture was flushed with $N_2$, filtered over a celite plug and concentrated *in vacuo*. The crude product was purified by silica gel column chromatography (DCM/Methanol 100:1→70:30) to obtain **8** (12 mg, 47 µmol, 96%) as a white solid. $^1$H NMR (600 MHz, MeOD) $\delta$ 4.15 (t, $J$ = 4.6 Hz, 1H, CH-1), 3.94 (dd, $J$ = 10.9, 3.2 Hz, 1H, CH-7B), 3.74 (dd, $J$ = 10.9, 3.1 Hz, 1H, CH-7A), 3.67 (dd, $J$ = 11.0, 4.8 Hz, 1H, CH-6), 3.64 (t, $J$ = 9.4 Hz, 1H, CH-3), 3.54 (dd, $J$ = 9.6, 4.5 Hz, 1H, CH-2), 3.34 – 3.29 (m, 2H, MeOD, CH-4), 2.00 (tt, $J$ = 11.1, 3.1 Hz, 1H, CH-5). $^{13}$C NMR (151 MHz, MeOD) $\delta$ 75.0 (C-3), 72.1 (C-2), 70.9 (C-4), 63.4 (C-1), 59.3 (C-7), 56.1 (C-6), 46.1 (C-5). HRMS: calcd. for $[C_7H_{15}N_2O_6S]^+$ 255.06453; found 255.06425.

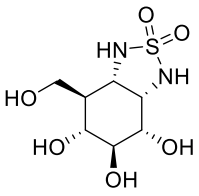

## 2.6 References


(1) Lombard, V.; Golaconda Ramulu, H.; Drula, E.; Coutinho, P. M.; Henrissat, B. The Carbohydrate-Active Enzymes Database (CAZy) in 2013. *Nucleic Acids Res.* **2014**, *42* (D1), 490–495.

(2) Hoefsloot, L. H.; Hoogeveen-Westerveld, M.; Reuser, A. J.; Oostra, B. A. Characterization of the Human Lysosomal Alpha-Glucosidase Gene. *Biochem. J.* **1990**, *272* (2), 493–497.

(3) HERS, H. G. Alpha-Glucosidase Deficiency in Generalized Glycogenstorage Disease (Pompe's Disease). *Biochem. J.* **1963**, *86* (1), 11–16.

(4) Lim, J.-A.; Li, L.; Raben, N. Pompe Disease: From Pathophysiology to Therapy and Back Again. *Front. Aging Neurosci.* **2014**, *6*, 177.

(5) McIntosh, P. T.; Hobson-Webb, L. D.; Kazi, Z. B.; Prater, S. N.; Banugaria, S. G.; Austin, S.; Wang, R.; Enterline, D. S.; Frush, D. P.; Kishnani, P. S. Neuroimaging Findings in Infantile Pompe Patients Treated with Enzyme Replacement Therapy. *Mol. Genet. Metab.* **2018**, *123* (2), 85–91.

(6) Güngör, D.; Reuser, A. J. J. How to Describe the Clinical Spectrum in Pompe Disease? *American journal of medical genetics. Part A*. United States February 2013, pp 399–400.

(7) DeRuisseau, L. R.; Fuller, D. D.; Qiu, K.; DeRuisseau, K. C.; Donnelly, W. H.; Mah, C.; Reier, P. J.; Byrne, B. J. Neural Deficits Contribute to Respiratory Insufficiency in Pompe Disease. *Proc. Natl. Acad. Sci.* **2009**, *106* (23), 9419–9424.

(8) Meena, N. K.; Raben, N. Pompe Disease: New Developments in an Old Lysosomal Storage Disorder. *Biomolecules* **2020**, *10* (9).

(9) Nicolino, M.; Byrne, B.; Wraith, J. E.; Leslie, N.; Mandel, H.; Freyer, D. R.; Arnold, G. L.; Pivnick, E. K.; Ottinger, C. J.; Robinson, P. H.; Loo, J.-C. A.; Smitka, M.; Jardine, P.; Tatò, L.; Chabrol, B.; McCandless, S.; Kimura, S.; Mehta, L.; Bali, D.; Skrinar, A.; Morgan, C.; Rangachari, L.; Corzo, D.; Kishnani, P. S. Clinical Outcomes after Long-Term Treatment with Alglucosidase Alfa in Infants and Children with Advanced Pompe Disease. *Genet. Med.* **2009**, *11* (3), 210–219.

(10) Fukuda, T.; Ahearn, M.; Roberts, A.; Mattaliano, R. J.; Zaal, K.; Ralston, E.; Plotz, P. H.; Raben, N. Autophagy and Mistargeting of Therapeutic Enzyme in Skeletal Muscle in Pompe Disease. *Mol. Ther.* **2006**, *14* (6), 831–839.

(11) Lim, J.-A.; Sun, B.; Puertollano, R.; Raben, N. Therapeutic Benefit of Autophagy Modulation in Pompe Disease. *Mol. Ther.* **2018**, *26* (7), 1783–1796.

(12) Banugaria, S. G.; Prater, S. N.; Patel, T. T.; DeArmey, S. M.; Milleson, C.; Sheets, K. B.; Bali, D. S.; Rehder, C. W.; Raiman, J. A. J.; Wang, R. A.; Labarthe, F.; Charrow, J.; Harmatz, P.; Chakraborty, P.; Rosenberg, A. S.; Kishnani, P. S. Algorithm for the Early Diagnosis and Treatment of Patients with Cross Reactive Immunologic Material-Negative Classic Infantile Pompe Disease: A Step towards Improving the Efficacy of ERT. *PLoS One* **2013**, *8* (6), e67052.

(13) van Gelder, C.; Kroos, M.; Özkan, L.; Plug, I.; Reuser, A.; van der Ploeg, A. Antibody Formation to Enzyme Therapy in Classic Infantile Pompe Disease: Implications of Patient Age. *BMC Musculoskelet. Disord.* **2013**, *14* (2), P18.

(14) Flanagan, J. J.; Rossi, B.; Tang, K.; Wu, X.; Mascioli, K.; Donaudy, F.; Tuzzi, M. R.; Fontana, F.; Cubellis, M. V.; Porto, C.; Benjamin, E.; Lockhart, D. J.; Valenzano, K. J.; Andria, G.; Parenti, G.; Do, H. V. The Pharmacological Chaperone 1-Deoxynojirimycin Increases the Activity and Lysosomal Trafficking of Multiple Mutant Forms of Acid Alpha-Glucosidase. *Hum. Mutat.* **2009**, *30* (12), 1683–1692.

(15) Porto, C.; Cardone, M.; Fontana, F.; Rossi, B.; Tuzzi, M. R.; Tarallo, A.; Barone, M. V.; Andria, G.; Parenti, G. The Pharmacological Chaperone N-Butyldeoxynojirimycin Enhances Enzyme Replacement Therapy in Pompe Disease Fibroblasts. *Mol. Ther.* **2009**, *17* (6), 964–971.

(16) Kishnani, P.; Tarnopolsky, M.; Roberts, M.; Sivakumar, K.; Dasouki, M.; Dimachkie, M. M.; Finanger, E.; Goker-Alpan, O.; Guter, K. A.; Mozaffar, T.; Pervaiz, M. A.; Laforet, P.; Levine, T.; Adera, M.; Lazauskas, R.; Sitaraman, S.; Khanna, R.; Benjamin, E.; Feng, J.; Flanagan, J. J.; Barth, J.; Barlow, C.; Lockhart, D. J.; Valenzano, K. J.; Boudes, P.; Johnson, F. K.; Byrne, B. Duvoglustat HCl Increases Systemic and Tissue Exposure of Active Acid α-Glucosidase in Pompe Patients Co-Administered with Alglucosidase α. *Mol. Ther.* **2017**, *25* (5), 1199–1208.

(17) Meena, N. K.; Ralston, E.; Raben, N.; Puertollano, R. Enzyme Replacement Therapy Can Reverse Pathogenic Cascade in Pompe Disease. *Mol. Ther. Methods Clin. Dev.* **2020**, *18*, 199–214.

(18) Khanna, R.; Powe, A. C. J.; Lun, Y.; Soska, R.; Feng, J.; Dhulipala, R.; Frascella, M.; Garcia, A.; Pellegrino, L. J.; Xu, S.; Brignol, N.; Toth, M. J.; Do, H. V; Lockhart, D. J.; Wustman, B. A.; Valenzano, K. J. The Pharmacological Chaperone AT2220 Increases the Specific Activity and Lysosomal Delivery of Mutant Acid Alpha-Glucosidase, and Promotes Glycogen Reduction in a Transgenic Mouse Model of Pompe Disease. *PLoS One* **2014**, *9* (7), e102092.

(19) Blair, H. A. Cipaglucosidase Alfa: First Approval. *Drugs* **2023**, *83* (8), 739–745.

(20) Andersson, U.; Butters, T. D.; Dwek, R. A.; Platt, F. M. N-Butyldeoxygalactonojirimycin: A More Selective Inhibitor of Glycosphingolipid Biosynthesis than N-Butyldeoxynojirimycin, in Vitro and in Vivo. *Biochem. Pharmacol.* **2000**, *59* (7), 821–829.

(21) Porto, C.; Ferrara, M. C.; Meli, M.; Acampora, E.; Avolio, V.; Rosa, M.; Cobucci-Ponzano, B.; Colombo, G.; Moracci, M.; Andria, G.; Parenti, G. Pharmacological Enhancement of α-Glucosidase by the Allosteric Chaperone N-Acetylcysteine. *Mol. Ther.* **2012**, *20* (12), 2201–2211.

(22) Roig-Zamboni, V.; Cobucci-Ponzano, B.; Iacono, R.; Ferrara, M. C.; Germany, S.; Bourne, Y.; Parenti, G.; Moracci, M.; Sulzenbacher, G. Structure of Human Lysosomal Acid α-Glucosidase-A Guide for the Treatment of Pompe Disease. *Nat. Commun.* **2017**, *8*, 1111.

(23) Marugan, J. J.; Zheng, W.; Motabar, O.; Southall, N.; Goldin, E.; Sidransky, E.; Aungst, R. A.; Liu, K.; Sadhukhan, S. K.; Austin, C. P. Evaluation of 2-Thioxo-2,3,5,6,7,8-Hexahydropyrimido[4,5-d]Pyrimidin-4(1H)-One Analogues as GAA Activators. *Eur. J. Med. Chem.* **2010**, *45* (5), 1880–1897.

(24) Kato, A.; Nakagome, I.; Hata, M.; Nash, R. J.; Fleet, G. W. J.; Natori, Y.; Yoshimura, Y.; Adachi, I.; Hirono, S. Strategy

for Designing Selective Lysosomal Acid α-Glucosidase Inhibitors: Binding Orientation and Influence on Selectivity. *Molecules* **2020**, *25* (12).

(25) Kato, A.; Nakagome, I.; Kanekiyo, U.; Lu, T.-T.; Li, Y.-X.; Yoshimura, K.; Kishida, M.; Shinzawa, K.; Yoshida, T.; Tanaka, N.; Jia, Y.-M.; Nash, R. J.; Fleet, G. W. J.; Yu, C.-Y. 5-C-Branched Deoxynojirimycin: Strategy for Designing a 1-Deoxynojirimycin-Based Pharmacological Chaperone with a Nanomolar Affinity for Pompe Disease. *J. Med. Chem.* **2022**, *65* (3), 2329–2341.

(26) Artola, M.; Wu, L.; Ferraz, M.; Kuo, C.-L.; Raich, L.; Breen, I.; Offen, W.; Codée, J.; van der Marel, G.; Rovira, C.; Aerts, J.; Davies, G.; Overkleeft, H. 1,6-Cyclophellitol Cyclosulfates: A New Class of Irreversible Glycosidase Inhibitor. *ACS Cent. Sci.* **2017**, *3* (7), 784–793.

(27) Beenakker, T. J. M.; Wander, D. P. A.; Offen, W. A.; Artola, M.; Raich, L.; Ferraz, M. J.; Li, K. Y.; Houben, J. H. P. M.; Van Rijssel, E. R.; Hansen, T.; Van Der Marel, G. A.; Codée, J. D. C.; Aerts, J. M. F. G.; Rovira, C.; Davies, G. J.; Overkleeft, H. S. Carba-Cyclophellitols Are Neutral Retaining-Glucosidase Inhibitors. *J. Am. Chem. Soc.* **2017**, *139* (19), 6534–6537.

(28) Artola, M.; Hedberg, C.; Rowland, R. J.; Raich, L.; Kytidou, K.; Wu, L.; Schaaf, A.; Ferraz, M. J.; Van Der Marel, G. A.; Codée, J. D. C.; Rovira, C.; Aerts, J. M. F. G.; Davies, G. J.; Overkleeft, H. S. α-d-Gal-Cyclophellitol Cyclosulfamidate Is a Michaelis Complex Analog That Stabilizes Therapeutic Lysosomal α-Galactosidase A in Fabry Disease. *Chem. Sci.* **2019**, *10* (40), 9233–9243.

(29) Serrano, P.; Llebaria, A.; Delgado, A. An Unexpected Chelation-Controlled Yb(OTf)3-Catalyzed Aminolysis and Azidolysis of Cyclitol Epoxides. *J. Org. Chem.* **2002**, *67* (20), 7165–7167.

(30) Chiasson, J.-L.; Josse, R. G.; Gomis, R.; Hanefeld, M.; Karasik, A.; Laakso, M. Acarbose for Prevention of Type 2 Diabetes Mellitus: The STOP-NIDDM Randomised Trial. *Lancet* **2002**, *359* (9323), 2072–2077.

(31) Scott, L. J.; Spencer, C. M. Miglitol. *Drugs* **2000**, *59* (3), 521–549.

(32) Larsbrink, J.; Izumi, A.; Hemsworth, G. R.; Davies, G. J.; Brumer, H. Structural Enzymology of Cellvibrio Japonicus Agd31B Protein Reveals Transglucosylase Activity in Glycoside Hydrolase Family 31. *J. Biol. Chem.* **2012**, *287* (52), 43288–43299.

(33) Hermans, M. M. P.; Krooss, M. A.; van Beeurnens, J.; Oostras, B. A.; Reusersll, A. J. J. Human Lysosomal A-Glucosidase Characterization of the Catalytic Site. *Biochemistry* **1991**, *266* (21), 13507–13512.

(34) Oude Elferink, R. P.; Van Doorn-Van Wakeren, J.; Strijland, A.; Reuser, A. J.; Tager, J. M. Biosynthesis and Intracellular Transport of Alpha-Glucosidase and Cathepsin D in Normal and Mutant Human Fibroblasts. *Eur. J. Biochem.* **1985**, *153* (1), 55–63.

(35) Oude Elferink, R. P. J.; van Doorn-van Wakereb, J.; Hendriks, T.; Strijland, A.; Tager, J. M. Transport and Processing of Endocytosed Lysosomal α-Glucosidase in Cultured Human Skin Fibroblasts. *Eur. J. Biochem.* **1986**, *158* (2), 339–344.

(36) Artola, M.; Kuo, C.-L.; Lelieveld, L. T.; Rowland, R. J.; Van Der Marel, G. A.; Codée, J. D. C.; Boot, R. G.; Davies, G. J.; Aerts, J. M. F. G.; Overkleeft, H. S. Functionalized Cyclophellitols Are Selective Glucocerebrosidase Inhibitors and Induce a Bona Fide Neuropathic Gaucher Model in Zebrafish. *J. Am. Chem. Soc.* **2019**, *141* (10), 4214–4218.

(37) Kabsch, W. XDS. *Acta Crystallogr. D. Biol. Crystallogr.* **2010**, *66*, 125–132.

(38) Winn, M. D.; Ballard, C. C.; Cowtan, K. D.; Dodson, E. J.; Emsley, P.; Evans, P. R.; Keegan, R. M.; Krissinel, E. B.; Leslie, A. G. W.; McCoy, A.; McNicholas, S. J.; Murshudov, G. N.; Pannu, N. S.; Potterton, E. A.; Powell, H. R.; Read, R. J.; Vagin, A.; Wilson, K. S. Overview of the CCP4 Suite and Current Developments. *Acta Crystallographica Section D: Biological Crystallography*. 2011, pp 235–242.

(39) Kovalevskiy, O.; Nicholls, R. A.; Long, F.; Carlon, A.; Murshudov, G. N. Overview of Refinement Procedures within REFMAC5: Utilizing Data from Different Sources. *Acta Crystallogr. Sect. D, Struct. Biol.* **2018**, *74* (Pt 3), 215–227.

(40) Lebedev, A. A.; Young, P.; Isupov, M. N.; Moroz, O. V.; Vagin, A. A.; Murshudov, G. N. JLigand: A Graphical Tool for the CCP4 Template-Restraint Library. *Acta Crystallogr. Sect. D Biol. Crystallogr.* **2012**, *68* (4), 431–440.

(41) Emsley, P.; Lohkamp, B.; Scott, W. G.; Cowtan, K. Features and Development of Coot. *Acta Crystallogr. Sect. D Biol. Crystallogr.* **2010**, *66* (4), 486–501.

(42) Williams, C. J.; Headd, J. J.; Moriarty, N. W.; Prisant, M. G.; Videau, L. L.; Deis, L. N.; Verma, V.; Keedy, D. A.; Hintze, B. J.; Chen, V. B.; Jain, S.; Lewis, S. M.; Arendall III, W. B.; Snoeyink, J.; Adams, P. D.; Lovell, S. C.; Richardson, J. S.; Richardson, D. C. MolProbity: More and Better Reference Data for Improved All-Atom Structure Validation. *Protein Sci.* **2018**, *27* (1), 293–315.

(43) Winter, G. Xia2: An Expert System for Macromolecular Crystallography Data Reduction. *J. Appl. Crystallogr.* **2010**, *43* (1), 186–190.

(44) Murshudov, G. N.; Skubák, P.; Lebedev, A. A.; Pannu, N. S.; Steiner, R. A.; Nicholls, R. A.; Winn, M. D.; Long, F.; Vagin, A. A. REFMAC5 for the Refinement of Macromolecular Crystal Structures. *Acta Crystallogr. Sect. D Biol. Crystallogr.* **2011**, *67* (4), 355–367.

(45) Emsley, P.; Cowtan, K. Coot: Model-Building Tools for Molecular Graphics. *Acta Crystallogr. Sect. D Biol. Crystallogr.* **2004**, *60* (12 I), 2126–2132.

(46) Jiang, J.; Kuo, C. L.; Wu, L.; Franke, C.; Kallemeijn, W. W.; Florea, B. I.; Van Meel, E.; Van Der Marel, G. A.; Codée, J. D. C.; Boot, R. G.; Davies, G. J.; Overkleeft, H. S.; Aerts, J. M. F. G. Detection of Active Mammalian GH31 α-Glucosidases in Health and Disease Using in-Class, Broad-Spectrum Activity-Based Probes. *ACS Cent. Sci.* **2016**, *2* (5), 351–358.

(47) Witte, M. D.; Kallemeijn, W. W.; Aten, J.; Li, K. Y.; Strijland, A.; Donker-Koopman, W. E.; van den Nieuwendijk, A. M. C. H.; Bleijlevens, B.; Kramer, G.; Florea, B. I.; Hooibrink, B.; Hollak, C. E. M.; Ottenhoff, R.; Boot, R. G.; van der Marel, G. A.; Overkleeft, H. S.; Aerts, J. M. F. G. Ultrasensitive in Situ Visualization of Active Glucocerebrosidase Molecules. *Nat. Chem. Biol.* **2010**, *6* (12), 907–913.

(48) Rowland, R. J.; Chen, Y.; Breen, I.; Wu, L.; Offen, W. A.; Beenakker, T. J.; Su, Q.; Nieuwendijk, A. M. C. H.; Aerts,

J. M. F. G.; Artola, M.; Overkleeft, H. S.; Davies, G. J. Design, Synthesis and Structural Analysis of Glucocerebrosidase Imaging Agents. *Chem. – A Eur. J.* **2021**, *27* (66), 16377–16388.

(49) Li, K. Y.; Jiang, J.; Witte, M. D.; Kallemeijn, W. W.; Van Den Elst, H.; Wong, C. S.; Chander, S. D.; Hoogendoorn, S.; Beenakker, T. J. M.; Codée, J. D. C.; Aerts, J. M. F. G.; Van Der Marel, G. A.; Overkleeft, H. S. Synthesis of Cyclophellitol, Cyclophellitol Aziridine, and Their Tagged Derivatives. *European J. Org. Chem.* **2014**, *2014* (27), 6030–6043.

(50) Schröder, S. P.; Wu, L.; Artola, M.; Hansen, T.; Offen, W. A.; Ferraz, M. J.; Li, K.-Y.; Aerts, J. M. F. G.; Van Der Marel, G. A.; Codée, J. D. C.; Davies, G. J.; Overkleeft, H. S. Gluco-1 H -Imidazole: A New Class of Azole-Type β-Glucosidase Inhibitor. *J. Am. Chem. Soc.* **2018**, *140* (15).

## 2.7 Appendix

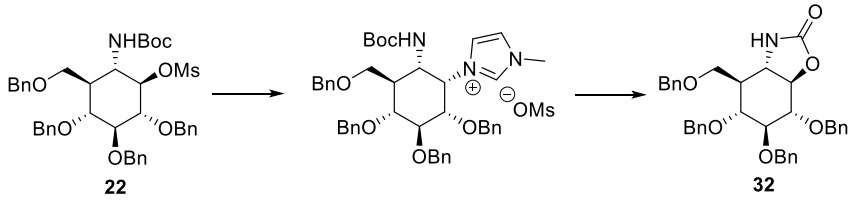


**Scheme S2.1.** Proposed side product formation due to double inversion.

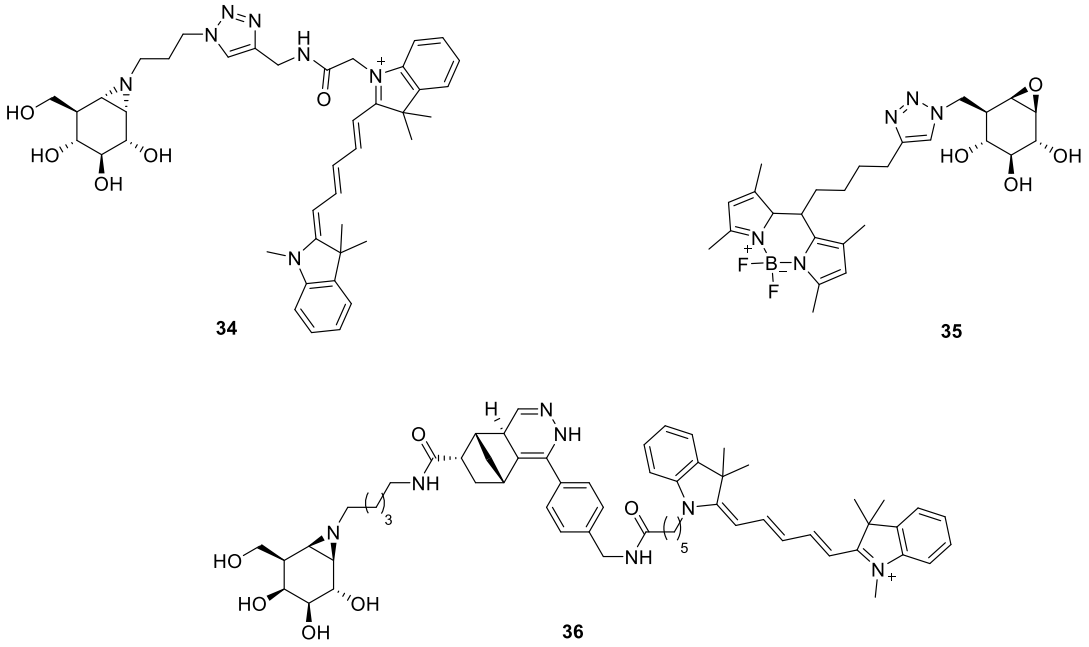


**Figure S2.1.** Structure of activity-based probes (ABPs) and inhibitors used in this Chapter: α-glucosidase ABP **34** (JJB383), selective GBA β-glucosidase ABP **35** (MDW933), α-galactosidase ABP **36** (TB652)

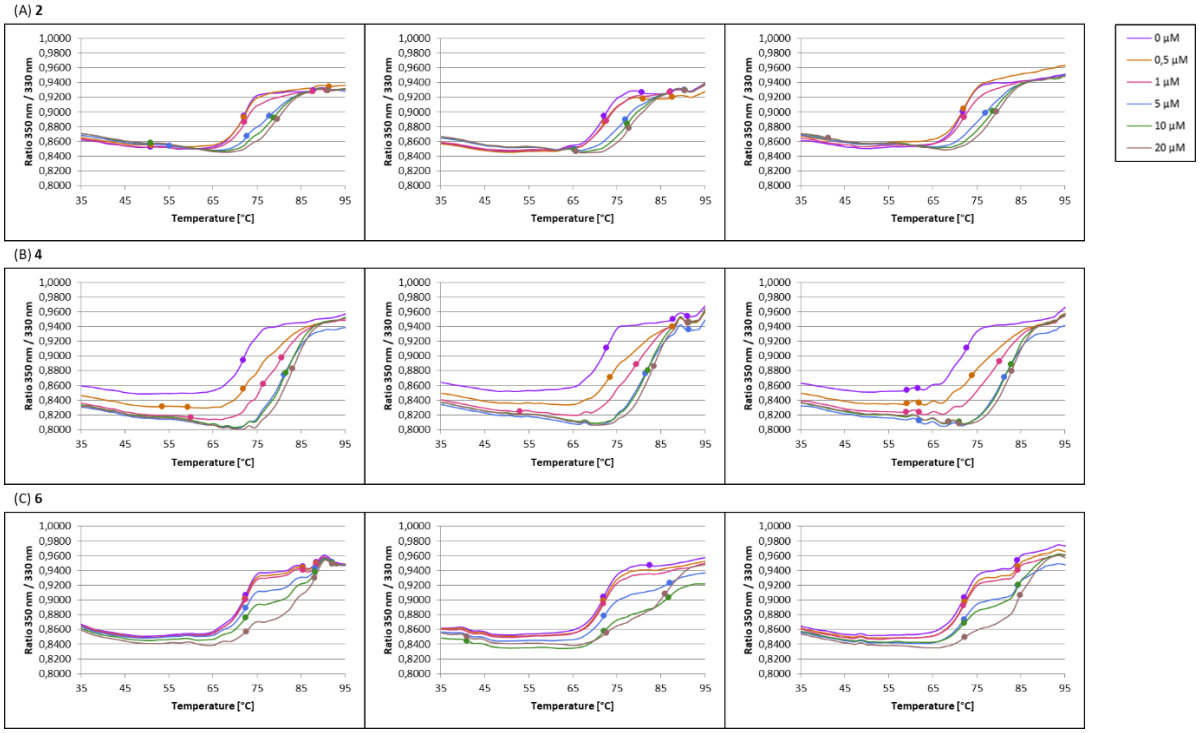


**Figure S2.2.** The unfolding curves measured by the Tycho NT-6 of Myozyme preincubated with 0 µM – 20 µM of compounds (A) **2**, (B) **4**, and (C) **6**.

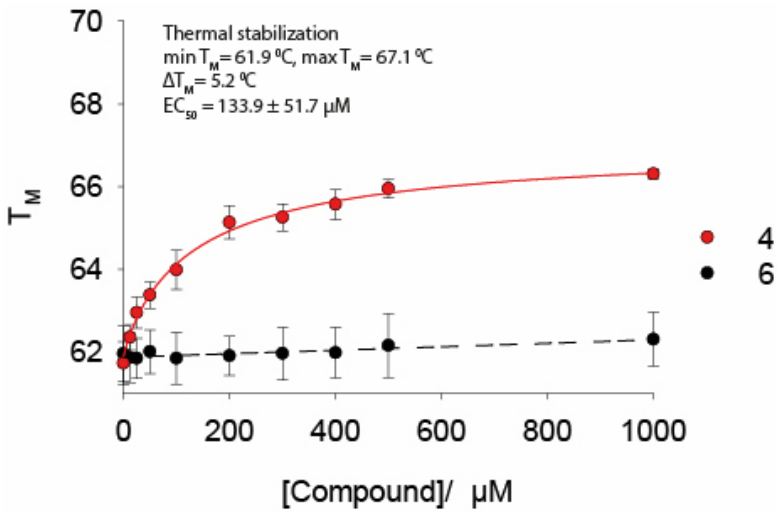


**Figure S2.3.** The effect of **4** and **6** on the thermostability of *Cj*Agd31B. Graph shows the heat-induced melting profiles of *Cj*Agd31B in complex with **4** (red) and **6** (black).